ORIGINAL PAPER

Non-stationarity, heterogeneity, scale effects, and anisotropy investigations on natural rock joint roughness using the variogram method

Pinnaduwa H. S. W. Kulatilake[1] · Shi-Gui Du[2] · Mawuko Luke Yaw Ankah[1] · Rui Yong[2] · Desmond Talamwin Sunkpal[1] · Xiaokang Zhao[1] · Guang-Jian Liu[3] · Rui Wu[1]

Abstract

The variogram method is used to investigate the effect of non-stationarity, heterogeneity, scale-related parameters and anisotropy on roughness quantification of a natural rock joint of size 1 m × 1 m. The methodology quantifies two parameters to capture the stationary roughness. The effect of the non-stationarity of the used profiles was found to be negligible on the computed fractal parameters. Calculated fractal parameter values reflected significant heterogeneity on one part of the roughness surface compared to the rest of the surface studied in the paper. Effect of joint size was found to be negligible on the calculated fractal parameter values. The authors believe that the controversial findings appear in the literature on scale effects have resulted from roughness heterogeneity, which has not been investigated in detail in the literature in quantifying roughness. Rock discontinuity surface showed major anisotropy with respect to roughness. Roughness in the direction along the axis of ridges and troughs (X-direction) of the joint surface was found to be significantly less compared to that in the direction perpendicular to the direction of axis of ridges and troughs. Thus, it agreed with the intuition that the discontinuity resulted from a shear fracture with the main shearing direction approximately parallel to the X direction.

Highlights

1. Roughness of a fairly large size (1 m × 1 m) natural rock joint is quantified.
2. Roughness heterogeneity, which is rarely addressed in the rock mechanics literature, is addressed in detail by performing more than 1700 computations.
3. Controversial findings appear in the literature on roughness scale effect due to joint size is clarified through systematic quantification and interpretation.
4. Roughness anisotropy is clearly shown for a discontinuity resulted from a natural shear fracture.
5. Reliability of the variogram technique as an accurate roughness quantification method is shown through more than 1700 consistent computations.

✉ Pinnaduwa H. S. W. Kulatilake
   kulatila@u.arizona.edu

[1] School of Resources and Environmental Engineering, Jiangxi University of Science and Technology, Ganzhou, Jiangxi 341000, People's Republic of China

[2] School of Civil and Environmental Engineering, Ningbo University, Ningbo, Zhejiang 315211, People's Republic of China

[3] Key Laboratory of Rock Mechanics and Geohazards of Zhejiang Province, Shaoxing University, Shaoxing, Zhejiang 312000, People's Republic of China

Introduction and literature review

Mechanical properties of rock joints depend very much on rock joint roughness (Barton 1973; Kulatilake et al. 1995). Hydraulic properties of rock joints are controlled by the void space distribution between the rough joint surfaces which is known as "aperture" distribution (Kulatilake et al. 2008). Accurate quantification of roughness is therefore important in estimating the mechanical and hydraulic properties of rock joints. The mechanical and hydraulic properties of rock joints in turn control the rock mass mechanical and hydraulic properties of most rock masses.

Surface roughness of rock joints has been measured using either the contact or non-contact methods. In the contact

methods, in taking measurements, there is physical contact either between the operator and the rock joint surface or between the instrument and the joint surface. Typical examples for contact methods are the compass/disc clinometer and linear profiling methods (Fecker and Rengers 1971), the shadow profilometry method (Maerz et al. 1990), mechanical or electronic stylus profilometry (Brown and Scholz 1985; Aydan et al. 1996; Du 1998; Develi et al. 2001; Du et al. 2009), and the tangent plane sampling and pin sampling technique (Rasouli and Harrison 2000). Even though the contact methods are relatively cheaper than the non-contact methods, they are time consuming and may not provide data at a high resolution for accurate roughness quantification. In the non-contact methods, the measurements are done without physically touching fracture surfaces. Laser profilometry (Huang et al. 1992; Hsiung et al. 1993; Brown 1995; Kulatilake et al. 1995; 2006; Xie et al. 1997; Belem et al. 2000; Jiang et al. 2006), laser scanning (Lanaro et al. 1998; Feng et al. 2003; Fardin et al. 2004; Ge et al. 2014; Yong et al. 2018), and stereo topometric cameras (Grasselli et al. 2002; Hong et al. 2008) are examples for non-contact methods. These non-contact methods provide many data at a high resolution within a short time. Rock joint roughness data obtained from a laser scanner is used in this paper to quantify rock joint roughness.

To quantify rock joint surface roughness, several methods have been proposed in the literature. The joint roughness coefficient (JRC) proposed by Barton (1973) has been widely used in engineering practice. It may be used in engineering practice as a preliminary index to assess roughness. However, several researchers have indicated shortcomings of JRC with respect to accurate quantification of rock joint roughness (Maerz et al. 1990; Miller et al. 1990; Hsiung et al. 1993; Kodikara and Johnston 1994; Kulatilake et al. 1995). Table 1 provides a list of statistical parameters or statistical functions, including the references, which have been suggested in the literature to quantify a roughness profile or a roughness surface. The parameters (1) through (3) given in Table 1 can be categorized as amplitude parameters of a roughness profile. The parameters or functions (4) through (15) given in Table 1 are various measures of either the slope or spatial variation of the roughness profile or roughness surface. The parameters (16) through (19) are measures of both the amplitude and slope or spatial variation of the roughness profile or roughness surface. Note that both the amplitude

Table 1 Statistical parameters and statistical functions suggested in the literature to quantify rock joint roughness

Roughness parameter number	Roughness parameter	Abbreviation	Reference(s)
1	Centerline average value of the profile	CLA	(Tse and Cruden 1979)
2	Mean square value of the profile	MSV	(Tse and Cruden 1979)
3	Root mean square value of the profile,	RMS	(Myers 1962; Tse and Cruden 1979)
4	Mean inclination angle of the profile	θ_P	(Yu and Vayssade 1991; Belem et al. 2000)
5	Mean positive inclination angle of the profile	θ_{P+}	Belem et al. (2000)
6	Mean negative inclination angle of the profile	θ_{P-}	Belem et al. (2000)
7	Standard deviation of the inclination angle of the profile	SD θ_P	(Yu and Vayssade 1991)
8	Root mean square of the slope of the profile	Z_2	(Myers 1962; Tse and Cruden 1979; Yu and Vayssade 1991)
9	Root mean square of the first derivative of the slope of the profile	Z_3	(Myers 1962; Tse and Cruden 1979)
10	Percentage excess distance measured along the profile where the slope is positive over the distance where the slope is negative	Z_4	(Myers 1962; Tse and Cruden 1979)
11	Auto correlation function	ACF	(Myers 1962; Wu and Ali 1978)
12	Structure function	SF	(Myers 1962; Sayles and Thomas 1977; Yu and Vayssade 1991)
13	Spectral density function	SDF	(Wu and Ali 1978)
14	Mean inclination angle for the surface	θ_S	Belem et al. (2000)
15	Root mean square of the slope of the surface	Z_{2S}	Belem et al. (2000)
16	Maximum apparent dip angle in the shear direction/an empirical roughness parameter + 1	$\theta_{Max}/C + 1$	(Grasselli et al. 2002; Tatone and Grasselli 2013)
17	Roughness profile index	R_P	(Mandelbrot 1967; Maerz et al. 1990; Yu and Vayssade 1991)
18	Surface roughness coefficient	R_S	(El−Soudani 1978; Belem et al. 2000)
19	Surface Tortuosity coefficient	T_S	Belem et al. (2000)

and a measure of slope are required to quantify roughness accurately (Kulatilake et al. 1995, 2006). Even though these statistical parameters or statistical functions have contributed to early development of roughness quantification, the value obtained for each of the afore-mentioned statistical parameters or values obtained for statistical functions depend on the sampling interval used for the computation. Therefore, for each statistical parameter or statistical function, several values or functions are possible depending on the selected sampling intervals. This fact leads to difficulty in assigning a unique value to quantify a roughness profile or surface. This is not a desirable feature for accurate roughness quantification. This led to investigation of other methods, which have scale invariant properties for all the scales or at least for a range of scales, to quantify rock joint roughness.

Both the self-similar and self-affine fractals have been suggested to use in quantifying rock joint roughness. The original divider (Mandelbrot 1967) and original box counting (Feder 1988) methods belong to self-similar fractals. The variogram (Orey 1970), spectral (Berry and Lewis 1980), roughness-length (Malinverno 1990), and the line scaling (Matsushita and Ouchi 1989) methods belong to self-affine fractals. The self-similar fractals provide scale invariant values for all the scales. On the other hand, the self-affine fractals provide scale invariant values only for a range of scales. Rock joint profiles belong to self-affine fractals (Russ 1994; Kulatilake et al. 1998; Ge et al. 2014). The original divider and the original box counting methods provide accurate results only for self-similar profiles. Kulatilake et al. (1997, 1998) and Kulatilake and Um (1999) explained the problems associated with using the original divider method in calculating correct fractal dimension values for self-affine profiles and modified the method to produce correct fractal dimension values. Kulatilake et al. (2006) extended this modified divider method to two dimensions and computed the fractal dimension and another fractal parameter, which is a measure of the amplitude of roughness, for a few natural rock joint surfaces.

Several researchers (Brown and Scholz 1985; Miller et al. 1990; Power and Tullis 1991; Poon et al. 1992; Huang et al. 1992; Odling 1994; Kulatilake et al. 1995, 1997, 1998, 2006; Shirono and Kulatilake 1997; Xie et al. 1997; Kulatilake and Um 1999; Fardin et al. 2001; Jiang et al. 2006) have quantified roughness of natural rock joints through self-affine fractals using the roughness length, variogram, spectral, or line scaling methods. An input parameter in a range of scale is used rather than a single value in computing fractal parameters using each of these methods. If the investigated roughness has a scale effect, different fractal parameter estimates can be computed through self-affine techniques by changing the range of scales. Therefore, the self-affine techniques may have better capabilities than statistical parameters or statistical functions in quantifying roughness accurately by reducing the sampling interval effect and accommodating

scale effects if they exist. The fractal dimension captures only the auto correlation of the roughness profile; a second fractal parameter is needed to capture the amplitude of the roughness profile (Kulatilake et al. 1995, 2006). All the afore-mentioned self-affine techniques can compute a fractal parameter which is a measure of the amplitude of the profile along with the fractal dimension (Kulatilake et al. 1995, 1997, 1998, 2006; Shirono and Kulatilake 1997; Kulatilake and Um 1999).

It has been shown in the literature (Miller et al. 1990; Huang et al. 1992; Kulatilake et al. 1995, 1997, 1998; Shirono and Kulatilake 1997; Kulatilake et al. 1999; Ge et al. 2014) that the fractal parameter values calculated by the roughness length, variogram, spectral, and line scaling methods may depend significantly on the input parameter value range used in each of those methods, as well as on the profile parameters such as stationary/non-stationary nature of the profile, data density (number of data per unit length), profile length, etc. After investigating the effect of the aforementioned factors on the accuracy of the fractal parameters estimated through the line scaling (Kulatilake et al. 1997), variogram (Kulatilake et al. 1998), roughness length (Kulatilake and Um 1999), and spectral (Shirono and Kulatilake 1997) methods, refined procedures have been suggested to quantify natural rock joint roughness accurately. These suggested guidelines indicate that one should use the self-affine methodologies in a careful manner to compute rock joint roughness accurately. These papers indicate that to obtain accurate fractal parameter estimates, the input parameter values should be selected in a certain narrow range. After performing research with all the self-affine methodologies, the first author of this paper recommended the variogram method as one of the best self-affine methods to quantify roughness accurately. Therefore, in this paper, the variogram technique is used with the suggested refined procedures (Kulatilake et al. 1998) to quantify natural rock joint roughness in two directions.

Please note that this paper limits the scale effect study only to rock joint roughness; it does not deal with the scale effects on rock joint mechanical properties. Several researchers have studied the effect of scale on the roughness of rock joints. Sample size, sampling interval used in the computation of statistical roughness parameters (or range of sampling intervals used in the computation of fractal roughness parameters), and measurement resolution of roughness have been considered in the previous studies of scale effects on joint roughness. Various conflicting conclusions (positive scale effect, negative scale effect, and no scale effect) have been reported in the literature on the roughness of rock joints with respect to sample size. Some studies (Bandis et al. 1981; Fardin et al. 2001, 2004; Cravero et al. 2001) reported a decreasing joint roughness with increasing joint sample size (termed as negative scale effect in this paper).

On the other hand, Leal-Gomes (2003) and Fardin (2008) have observed the joint roughness to increase with the joint sample size (termed as positive scale effect in this paper) in their studies. Swan and Zongi (1985), Maerz et al. (1990), and Cravero et al. (1995) have reported both positive and negative scale effects with sample size.

Xie et al. (1997) found that the rock joint sample size and measurement resolution of scanning equipment contribute to scale effect when variogram technique is used to quantify joint roughness. Based on their findings, the authors noted that as the sampling length increased, the fractal dimension (D) to increase and the amplitude-related parameter to decrease. Note that their maximum sample size was limited to only 150 mm. The authors thought that the inhomogeneity of the joint surfaces might have contributed to the scale effects arising due to the sample size. Both parameters were reported to decrease with decreasing measurement resolution (within 0.125 to 1 mm data spacing).

Tatone and Grasseli (2013) investigated the roughness scale dependency of rock joints using two large-scale in situ joint surfaces of areas approximately 4 and 6 m^2. The effect of measurement resolution on joint roughness was studied by taking measurements on small-scale joint specimens (100×100 mm^2) at various resolutions. Apart from the fractal dimension, on all other roughness parameters, they found a positive scale effect. They reported the resolution to have a stronger effect on roughness compared to the sample size. The authors asserted that the decrease in roughness with increasing sample size found by some researchers might have been a result of inconsistency in measurement resolution. The authors also observed, like authors such as Bandis et al. (1981), Xie et al. (1997), Lanaro et al. (1999), Lanaro (2000), and Fardin et al. (2001), that surface roughness values become constant beyond a threshold value as sample size increases.

The contradictory observations of previous studies clearly show that our understanding of scale effects on rock joint roughness is weak and inconclusive. These contradictory findings might have resulted partly due to not considering the factors such as heterogeneity and non-stationarity of rock joint surfaces play on the scale effects of rock joint roughness. Also, possibility exists for the contradictory findings to occur due to using inappropriate or inconsistent sampling intervals (or range of sampling intervals) or/and measurement resolutions in studying the scale effect on rock joint roughness. Therefore, a systematic, comprehensive study on the scale effects of joint roughness incorporating all the afore-mentioned factors (including heterogeneity and non-stationarity) and using a relatively large joint surface is badly needed. Such a study is performed as one part of the investigation in this paper using a 1 m × 1 m rock joint surface.

The rest of the introduction provides a literature review on anisotropic joint roughness. Kulatilake et al. (1995)

incorporated the anisotropic joint roughness in developing an anisotropic peak shear strength criterion for rock joints. Since then, several authors performed research on anisotropic joint roughness (Aydan et al. 1996; Xie et al. 1997; Kulatilake et al. 1999, 2006; Belem et al. 2000; Ge et al. 2014).

Aydan et al. (1996) reported anisotropy to be more evident in the tensile and shear fractures compared to the bedding planes. They pointed out that the results obtained were influenced mainly by the sampling interval and profile length. Xie et al. (1997) reported that due to joint surface anisotropy, the fractal dimension values obtained along the fracture propagation direction is generally lower than that obtained along the direction orthogonal to the fracture propagation. Belem et al. (2000) suggested a parameter known as degree of apparent anisotropy (Ka) to quantify roughness anisotropy; based on Ka values, a classification scheme (5 classes) which ranges from zero (anisotropic surface) to one (isotropic surface) was proposed for classifying anisotropic morphologies.

Ge et al. (2014) investigated the roughness of natural rock joints using two fractal methods (the variogram and modified 2-D divider); both linear profile roughness (2-D) and surface roughness (3-D) analyses were conducted using the two methods. In both methods, stationary roughness was described using the fractal dimension and an amplitude parameter. The results obtained using the two methods agreed well with each other. Anisotropy, which is inherent in rock joints, was also studied using three methods, the variogram, a triangular plate approach, and a light source approach. Results obtained using these three methods were also reported to be in good agreement.

Rock joint anisotropy is studied as the second part in this paper by applying the variogram technique, suggested by Kulatilake et al. (1998), on a rock joint surface of size 1 m × 1 m resulted from a shear fracture.

Rock joint surface acquisition and digitization of the joint surface roughness

Selection of rock joint surface from the field and its description

Heshangnong quarry is in Qingshi Town, southeast of Changshan County, Zhejiang Province, China, approximately 213.5 km south-west from Hangzhou city as shown in Fig. 1a (Yong et al. 2018; Du et al. 2021). The exploitation of this quarry required a pit with a length of 87 m, a width of 59 m, and a maximum height of 79 m (Fig. 1b). In this pit, the overburden mainly consists of calcareous slate, which originated from Ordovician argillaceous limestone under the condition of light
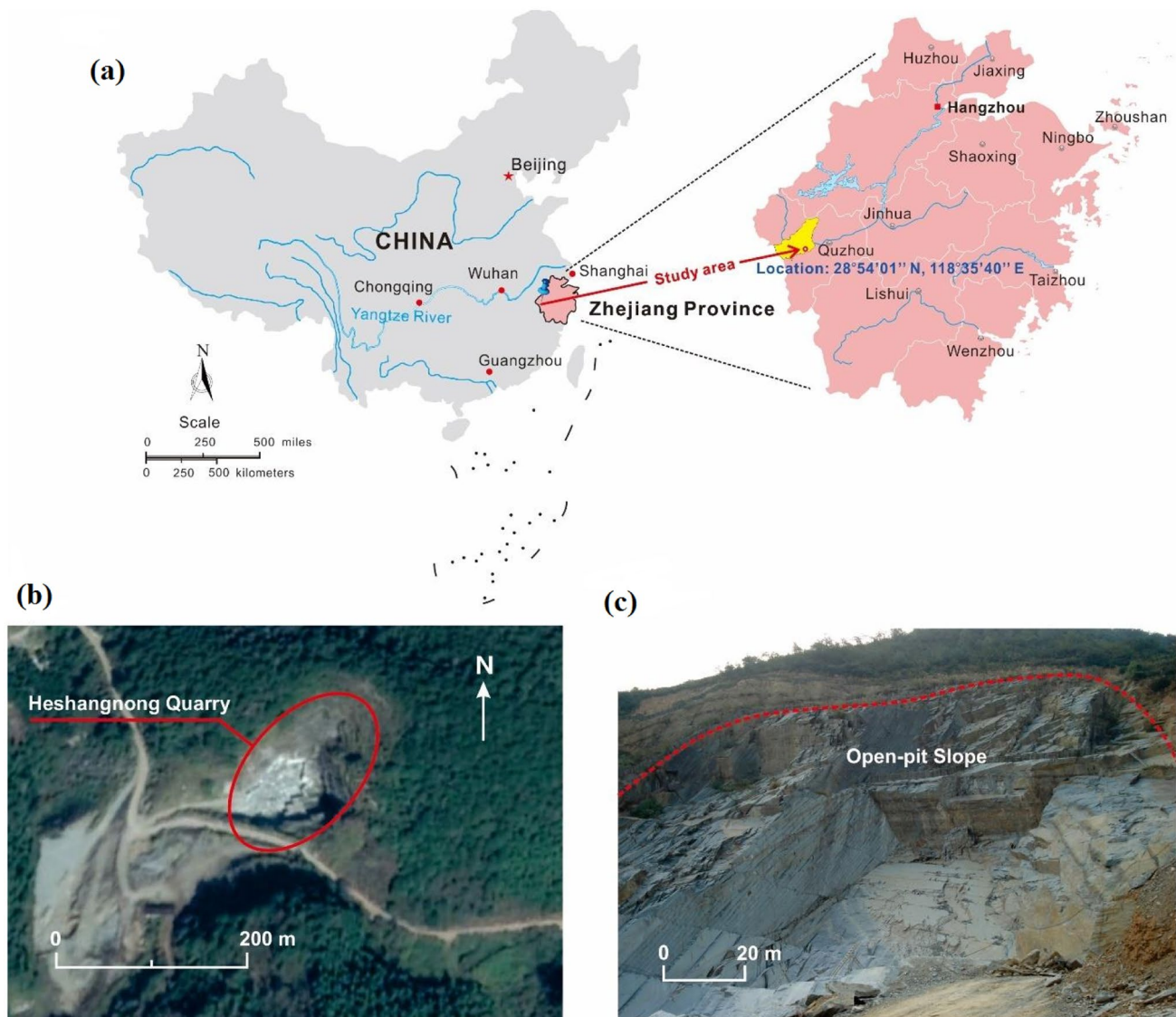
Fig. 1 Joint sample site (Yong et al. 2018; Du et al. 2021): **a** Location map, **b** satellite view of the Heshangnong Quarry, **c** view of the structurally controlled open-pit slope

metamorphism. The stability of this open pit is controlled by the foliations of the slate that generally dips about 55° to the SW. The grayish-green slate rock wall is foliated, very fine-grained, and formed by the metamorphosed intermediate tuff. The very distinct, continuous foliation planes in the overburden rock are oriented with strikes approximately parallel to the pit walls and dips toward the bottom of the pit (Fig. 1c).

To determine the morphological properties of rock joints at the laboratory and field scales, a sample with an overall area of 1100×1100 mm^2 (Fig. 2a) was sawed from the slate rock and transported to the laboratory. A study area with a size of 1000×1000 mm^2 was obtained from the central area of this sample to avoid the possible damaged edge areas of the sample during transport to the laboratory. The roughness is a measure of the inherent surface waviness and unevenness of a discontinuity

relative to its mean plane (ISRM 1978). A clear demarcation size between the unevenness and waviness does not exist in the literature. Waviness refers to the large-scale undulations of the surface topography measured over the lengths of meters, while unevenness refers to the small-scale surface topography encompassing asperities defined by sub-millimeter amplitudes measured over the lengths of centimeters. The selected joint sample size of 1000 mm × 1000 mm can be considered to cover only the unevenness part of the rock joint roughness.

Digitization of the joint surface roughness

A 3D laser scanning system, Metra Scan 750 (Fig. 2a), with a maximum accuracy of 0.030 mm, was used to measure the geometry of the joint surface (Yong et al. 2018). Its main
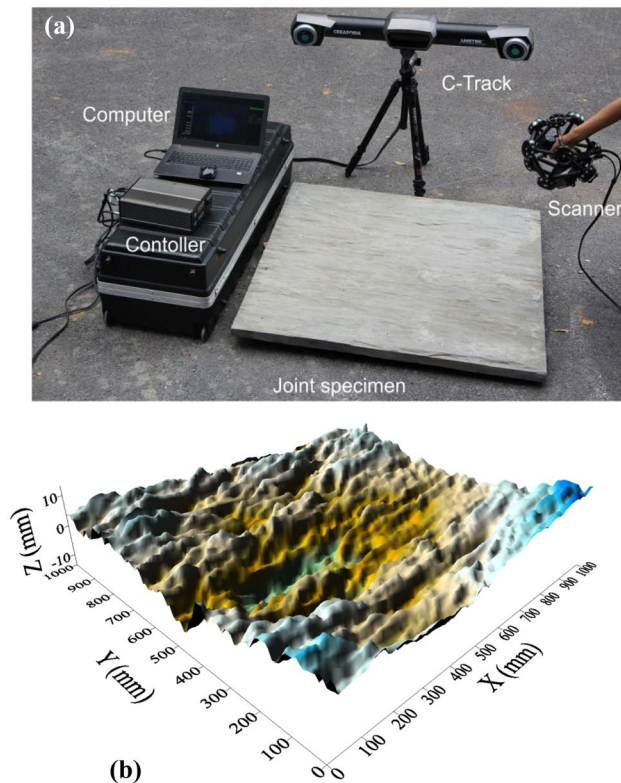
Fig. 2 Joint surface: **a** Scanning of the joint surface (Yong et al. 2018), **b** digitized joint surface (note that the scale is approximately reduced by 10 times in both the X and Y directions compared to the Z direction)

components include a scanner, C-Track cameras, a controller, and a computer. The surface acquisition was achieved by observing the paths of laser lines projected on the rock joint surface. As the lasers swept over the surface by the scanner, the scanner measured the 3D coordinates of the sample surface using seven laser paths, and the data were registered depending on the triangulated position. The final 3D surface model of the study area was obtained after point cloud data processing using the scanner software (Yong et al. 2018). It seems that a sampling interval of no more than 1 mm has the capability to capture the microfeatures of the surface morphology (Zhang et al. 2016). Therefore, surface roughness heights (Z) were digitized at a spacing of 0.5 mm in two perpendicular directions (X and Y). Note that X is visualized as the approximate shearing direction of the joint in the field. The measurement resolution of the spatial location of each point in the three-dimensional space along the X, Y, and Z directions is ± 0.10 mm. Figure 2b shows the rock joint surface resulted from the afore-mentioned digitized data. Note that the scale is approximately reduced by ten times in both the X and Y directions. In the Z direction, the scale is close to the actual surface height. Due to the different scales in X, Y, and Z directions, the roughness is approximately

exaggerated by ten times. Figure 2b shows that most of the axes of the ridges and troughs of the surface are approximately parallel to the X direction. Therefore, it is expected to have low roughness in the X direction and high roughness in the Y direction.

Main features of the variogram method

Let Z (X) be a Gaussian process with stationary increments and mean equaling 0. The variogram function of Z (X) is given by $2\gamma (X, h) = E [(Z (X + h)-Z(X))^2]$ where E stands for the expected value, and h is the lag distance along the X-axis. If $[2\gamma (X, h)]_{h \to 0}$ follows the power function given by Eq. (1), then the fractal dimension, D, of Z (X) is equal to 2-H, where H is the Hurst exponent (Orey 1970). In Eq. (1), K_v is a proportionality constant. Note that D and K_v are, respectively, the measures of the autocorrelation and amplitude of the roughness profile:

$$2\gamma(X,h)_{h\to 0} = K_v h^{2H} \tag{1}$$

Equation (1) can be written as Eq. (2) by taking the log of both sides of Eq. (1):

$$\log \left\{ [2\gamma(X, \, h)]_{h\to 0} \right\} = \log K_V + 2H \, \log \, h \tag{2}$$

To check whether Eq. (1) holds true, the linearity of the plot between log {(variogram) $_{h\to 0}$} and log (h) is checked by performing regression analysis; a resulting multiple linear correlation coefficient (R) value of greater than 0.85 confirms strong linearity. The slope of Eq. (2) provides 2H. D is then calculated from the expression D = 2-H. The intercept of Eq. (2) is equal to log K_v; this allows calculation of K_v. The variogram should be expressed in a discretized form so that it can be applied to the digitized roughness profile data. The discretized form of $2\gamma (X, h)$ is shown in Eq. (3), where X is the horizontal distance along a roughness profile and Z (X) is the height of the roughness profile from the datum.

$$2\gamma(X, h) = \frac{1}{M} \sum_{i=1}^{M} \left[Z(X_i) - Z(X_i + h) \right]^2 \tag{3}$$

in Eq. (3), M is the total number of pairs of roughness heights of the profile that are spaced at a lag distance h.

Kulatilake et al. (1998) pointed out that to calculate accurate fractal parameters through the variogram method, h needs to be in a certain range and that the range depends on the data density, d, and the D value of the profile. They came up with a conservative equation of $hd = 1.76$ to estimate the initial h value by knowing the d value of the profile to apply for profiles having unknown D values between 1.0 and 1.7. They recommended to compute six more h values using an increment factor of 1.2 starting from the estimated initial

h value, and then to use these seven h values in computing the corresponding 2γ (X, h) values and hence to plot log $(2\gamma$ $(X, h))$ vs. log (h) to check the strong linearity between the two parameters by obtaining a R value greater than 0.85, and then to estimate the D and K_v. Also, they suggested to use DxK_v (in here x stands for the multiplication symbol) as a parameter to combine the effect of D and K_v to a single roughness parameter. The above suggestions were strictly followed in calculating the fractal parameters D, K_v, and DxK_v included in this paper. Also, they stated that for the calculated fractal parameters to be accurate the roughness increments of the profiles should satisfy second order stationary requirements. Please note that the variogram procedure explained above is applicable to any size of sample covering from laboratory to field scales. In using $hd = 1.76$, d can be expressed per mm or cm for laboratory samples and per m for field samples.

Rock joint surface roughness quantification through the variogram technique

Effect of non-stationarity on computed D, K_v, and DxK_v of roughness profiles

Figure 2b shows the rock joint surface. Visually, it does not show significant inclination/declination of the roughness surface in either the Y-direction or in the X-direction. The same figure shows clearly that the profile undulations are less in the X-direction compared to the Y-direction. Figure 3a, b show a few roughness profiles in the X direction without and with removal of the global linear trend, respectively. Figure 3c, d show a few roughness profiles in the Y direction without and with removal of the global linear trend, respectively. Roughness data with removal of linear trend are known as "residual roughness" data in this paper. The raw roughness data are known simply as "roughness data" in this paper. These profiles clearly show that the roughness profiles in the X direction (termed as Z-X profiles from now onwards) have a lower inclination/declination trend and undulations compared to that of the profiles in the Y direction (termed as Z-Y profiles from now onwards). Therefore, if there is an effect of non-stationarity on computed D and K_v, it should show up more on the computational results of the Z-Y profiles compared to that of the Z-X profiles. Thus, it was decided to investigate the effect of the non-stationarity on the computed D, K_v, and DxK_v using the 1000 mm and 500 mm Z-Y profiles.

In the roughness profiles, the data are available at a spacing of 0.5 mm. Therefore, if mm is chosen as the unit, the data density, d, (the number of data per unit length) of each profile is 2. That means according to the condition of $hd = 1.76$, the minimum h to be used in the variogram

calculations should be greater than 0.88 (1.76/2). In this paper, seven values were used in calculating the early part of the variogram with the minimum h value selected at 1 mm and the increment set at 1.2 to obtain the remaining values. First, 1000 mm and 500 mm profiles were selected on the Z-Y planes at a spacing of 10 mm starting at X = 0.0 and ending at X = 1000 mm. This resulted in one hundred and one 1000 mm profiles and two hundred and two 500 mm profiles. The 500 mm profiles had two sets of equal number: (a) Y = 0 to 500 mm and (b) Y = 500 to 1000 mm. Each profile was subjected to regression analysis to obtain the global linear trend and then to find the residual roughness data profile. For 1000 mm and 500 mm profiles, the trend angle ranges of ($-0.008°$ to $+0.003°$) and ($-1.9°$ to $+1.0°$) were obtained, respectively. This indicates that the trend angles are very low for all the profiles. Variogram calculations were performed for each of the above-mentioned profiles using the procedure given in "Main features of the variogram method" under the following two cases: (a) raw roughness data and (b) residual roughness data. The obtained results are given in Figs. 4 and 5 and Table 2. Results are also given for the roughness profiles shown in Fig. 3c, d. Comparison of the results obtained for raw roughness data and residual roughness data clearly show that the non-stationarity resulting from a linear trend has no effect on the calculated roughness parameters for the investigated profiles. This means, for the studied joint surface, it is alright to use even raw roughness data for roughness parameter computations.

Effect of heterogeneity on computed D, K_v, and DxK_v of roughness profiles

The effect of heterogeneity on quantified roughness parameters either has not been dealt with or rarely addressed in the rock mechanics literature. On the other hand, the authors believe that the heterogeneity can play a major role in interpreting results on scale effect of roughness. The authors feel that for proper interpretation of effect of joint size on roughness, the roughness surface should be homogeneous. Results obtained on scale effect of roughness from heterogeneous surfaces can lead to misleading conclusions due to the influence of heterogeneity. Unfortunately, researchers have no control over the heterogeneity in dealing with natural rock joint roughness. Most probably in the past, heterogeneity might not have been considered at all in making interpretations of effect of joint size on roughness. This might have led to controversial findings that appear in the literature on scale effect of roughness. The following profiles were subjected to variogram calculations using the procedures given in "Main features of the variogram method" to investigate the effect of heterogeneity on calculated roughness parameters: (a) Z-X profiles of 1000 mm spaced at every 10 mm in the Y direction; (b) Z-X profiles of 500 mm (0–500 mm

Fig. 3 A few roughness profiles: **a** Z-X profiles without removal of trend, **b** Z-X profiles with removal of trend, **c** Z-Y profiles without removal of trend, and **d** Z-Y profiles with removal of trend
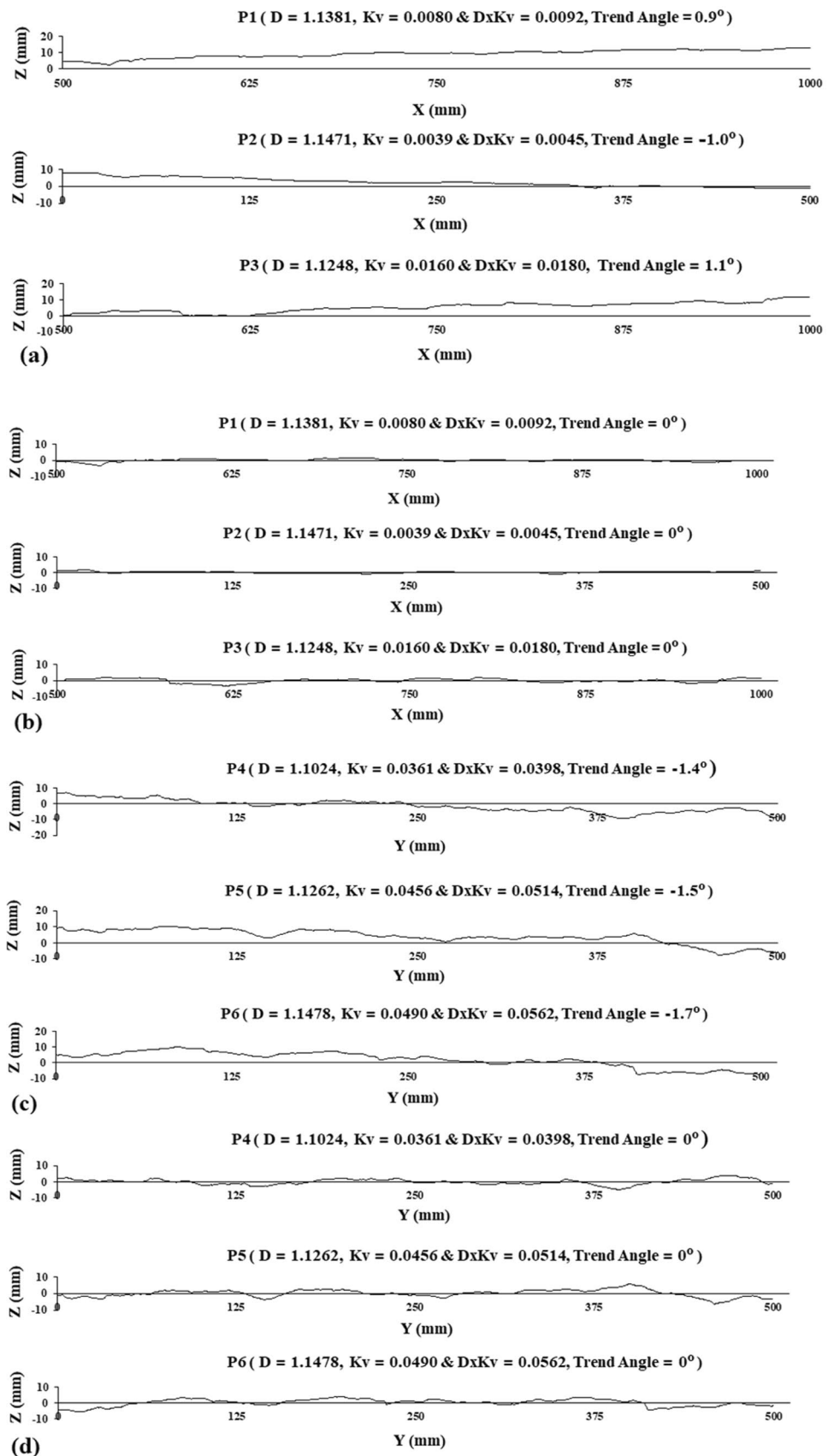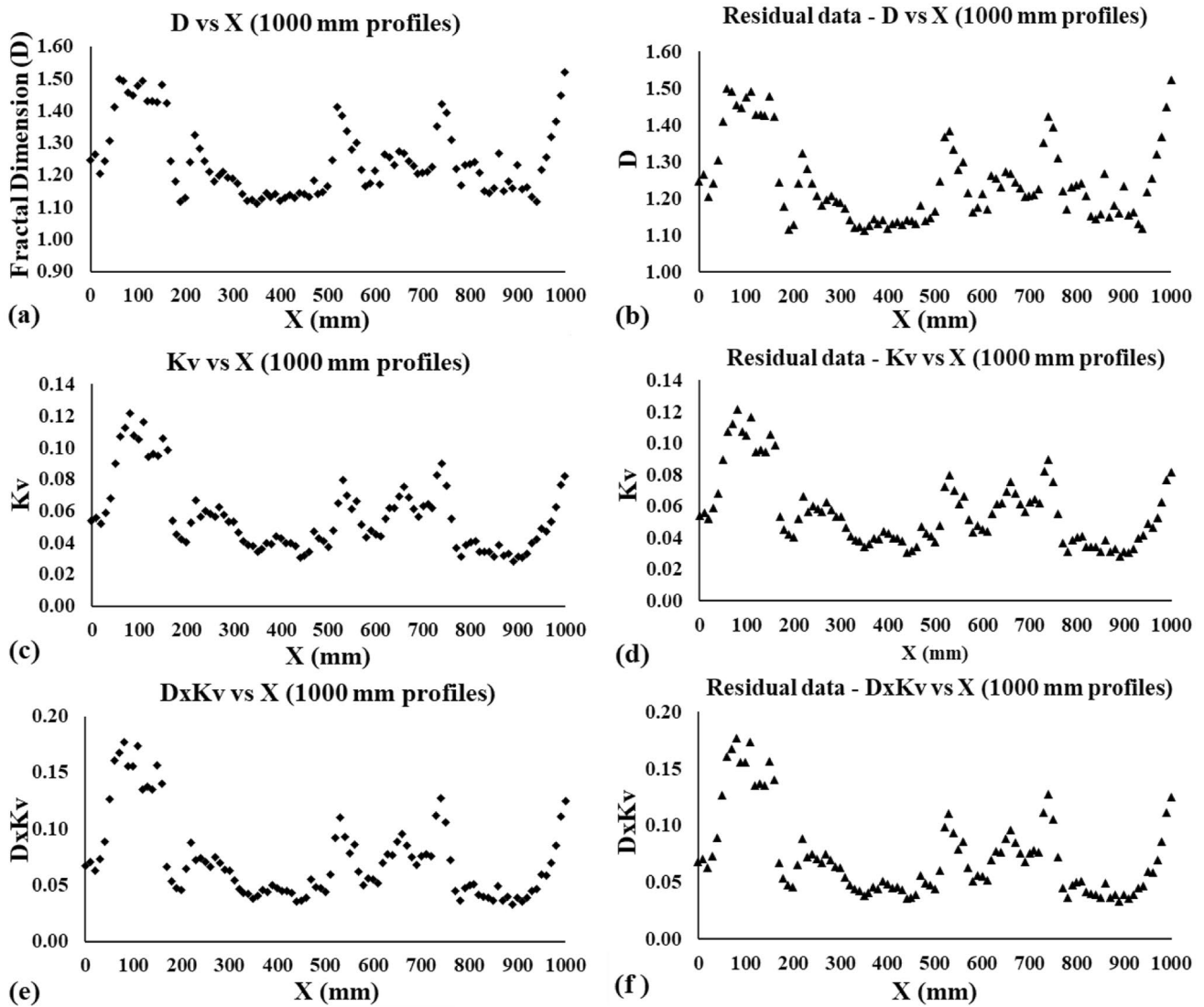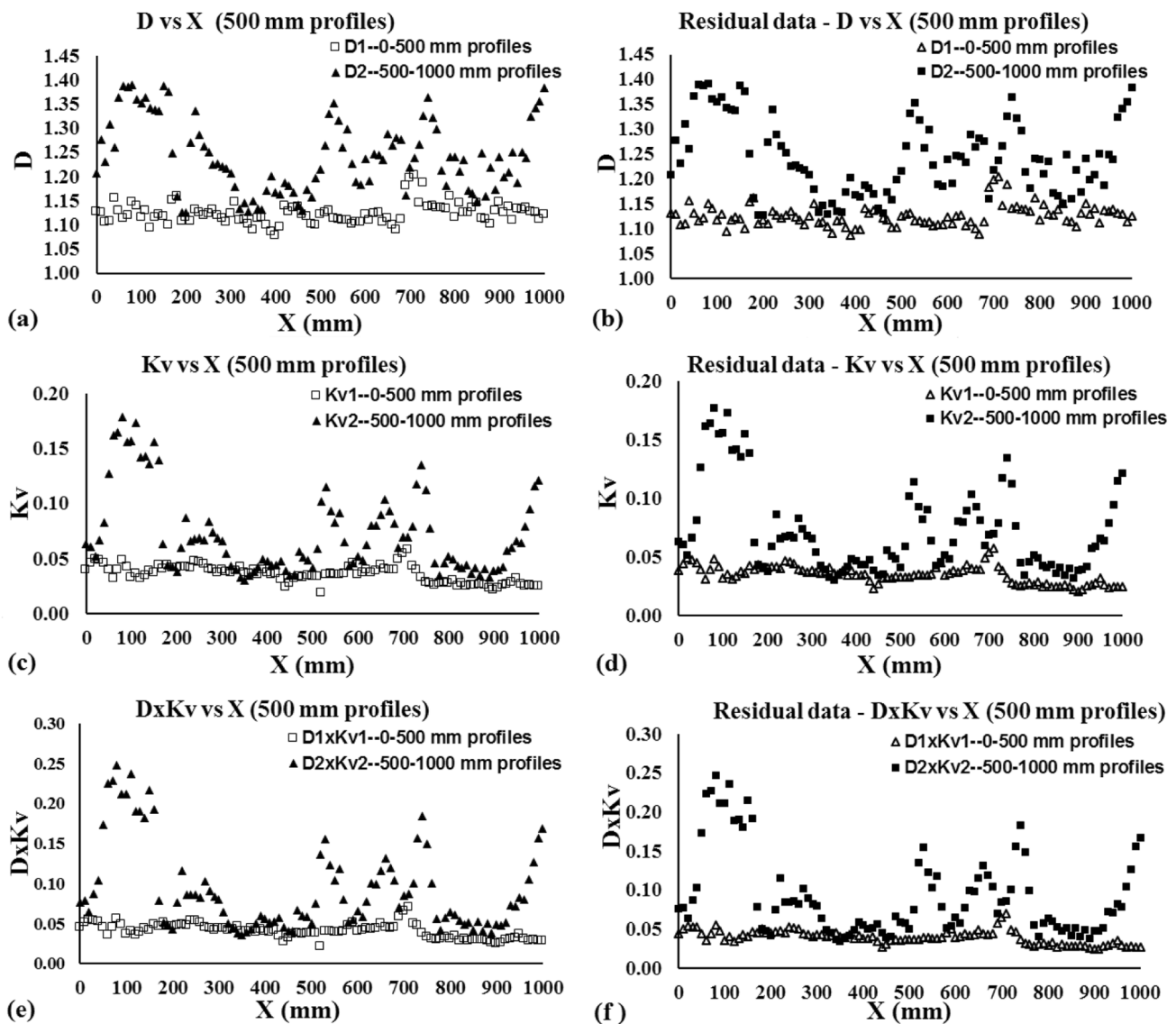
Fig. 4 Results obtained for different fractal parameters for 1000 mm Z-Y profiles: **a** D for raw roughness data; **b** D for residual roughness data; **c** K_v for raw roughness data; **d** K_v for residual roughness data; **e** DxK_v for raw roughness data, and **f** DxK_v for residual roughness data

and 500–1000 mm sections) spaced at every 10 mm in the Y direction; (c) Z-X profiles of 250 mm (0–250 mm, 250–500 mm, 500–750 mm, and 750–1000 mm sections) spaced at every 20 mm in the Y direction; (d) Z-X profiles of 125 mm (0–125 mm, 125–250 mm, 250–375 mm, 375–500 mm, 500–625 mm, 625–750 mm, 750–875 mm, and 875–1000 mm sections) spaced at every 40 mm in the Y direction; (e) Z-Y profiles of 1000 mm spaced at every 10 mm in the X direction; (f) Z-Y profiles of 500 mm (0–500 mm and 500–1000 mm sections) spaced at every 10 mm in the X direction; (g) Z-Y profiles of 250 mm (0–250 mm, 250–500 mm, 500–750 mm, and 750–1000 mm sections) spaced at every 10 mm in the X direction. The obtained results for the aforementioned (a) through (g) profile categories are shown in Figs. 6, 7, 8, 9, 10, 11, and

12, respectively. The summary statistics of the results for all the Z-X and Z-Y profiles are given in Tables 3 and 4, respectively. Note that for the 750–1000-mm section of the 250 mm Z-Y profiles, 23 of the 101 profiles produced *R* (linear correlation coefficient) values less than 0.85. Therefore, those results were not included in computing the summary statistics for this section (see Table 3). All other Z-Y profiles and all the Z-X profiles produced *R* values greater than 0.85.

For 250-mm Z-Y profiles, the roughness parameter values obtained for the section from 750 to 1000 mm show relatively higher values on the average and higher variability with respect to X values compared to that of the other three Sects. (0–250 mm, 250–500 mm, and 500–750 mm) (see Fig. 12 and Table 4). These results indicate that the Sects. 0–250 mm, 250–500 mm, and 500–750 mm of Z-Y

Fig. 5 Results obtained for different fractal parameters for 500 mm Z-Y profiles: **a** D for raw roughness data; **b** D for residual roughness data; **c** K_v for raw roughness data; **d** K_v for residual roughness data; **e** DxK_v for raw roughness data, and **f** DxK_v for residual roughness data

profiles can be considered as relatively homogeneous. On the other hand, the 750 to 1000-mm section of Z-Y profiles is highly heterogeneous compared to that of the 0–750 mm section of Z-Y profiles. For 500 mm Z-Y profiles, the roughness parameter values obtained for the section from 500 to 1000 mm show relatively higher values on the average and higher variability with respect to X values compared to that of the section from 0 to 500 mm (see Fig. 11 and Table 4). These results indicate that the 0–500 mm section of Z-Y profiles can be considered as relatively homogeneous. On the other hand, the 500 to 1000 mm section of Z-Y profiles is highly heterogeneous compared to that of the 0–500 mm section of Z-Y profiles. Higher values and higher variability for the 500–1000 mm section of Z-Y profiles compared to

the 0–500 mm section of Z-Y profiles have resulted from the higher values and higher variability of the 750–1000 mm section of Z-Y profiles. These observations very clearly show the consistency of the calculated values from the variogram method. For 1000 mm Z-Y profiles, the roughness parameter values show high variability with respect to X values (see Fig. 10). This high variability has resulted from the heterogeneity of the 750–1000 mm section of the Z-Y profiles compared to the 0–750 mm section of the Z-Y profiles. This again very clearly shows the consistency of the calculated values from the variogram method. The roughness parameter values obtained for Z-X profiles show significantly lower level of heterogeneity compared to that of the Z-Y profiles (see Figs. 6, 7, 8, and 9; Table 3).

Table 2 Roughness summary statistics of results used to investigate the effect of non-stationarity (resulting from a linear trend) on calculated variogram parameters

Case	No. of data	D			K_v			DxK_v		
		Mean	Range	CV	Mean	Range	CV	Mean	Range	CV
1000 mm Z-Y profiles Raw data	101	1.2458	1.1124–1.5199	0.0885	0.0564	0.0281–0.1213	0.3940	0.0725	0.0326–0.1766	0.4955
1000 mm Z-Y profiles Residual data	101	1.2457	1.1123–1.5229	0.0881	0.0565	0.0280–0.1213	0.3947	0.0726	0.0324–0.1766	0.4960
500 mm Z-Y profiles Raw data	202	1.1830	1.0782–1.3887	0.0685	0.0543	0.0188–0.1782	0.5995	0.0666	0.0212–0.2475	0.6974
500 mm Z-Y profiles Residual data	202	1.1848	1.0872–1.3907	0.0679	0.0540	0.0212–0.1777	0.6037	0.0663	0.0244–0.2471	0.7013

CV coefficient of variation

Effect of joint size on computed D, K_v, and DxK_v of roughness profiles

The "Effect of heterogeneity on computed D, Kv, and DxKv of roughness profiles" results showed that 0–500 mm section of Z-Y can be treated as a relatively homogeneous section. In addition, the results of the same section showed that 0–250 mm and 250–500 mm sections of Z-Y can be considered under one homogeneous section. First, these homogeneous sections are used to study the effect of joint size on the computed roughness parameters. Note that this eliminates the influence of heterogeneity on the effect of joint size on the computed roughness parameters. This is the first time any research group in the world has conducted such an analysis. Table 5 compares the summary results obtained for the roughness parameters between the lumped 0–250 mm and 250–500 mm sections of Z-Y profiles and the 0–500 mm section of Z-Y profiles. Table 5 shows that the mean values of D, K_v, and DxK_v are almost the same for the two categories; 250-mm sections show slightly higher variability compared to that of the 500-mm section due to a higher number of data. Note that these homogeneous sections of different sizes do not show the scale effect due to joint size.
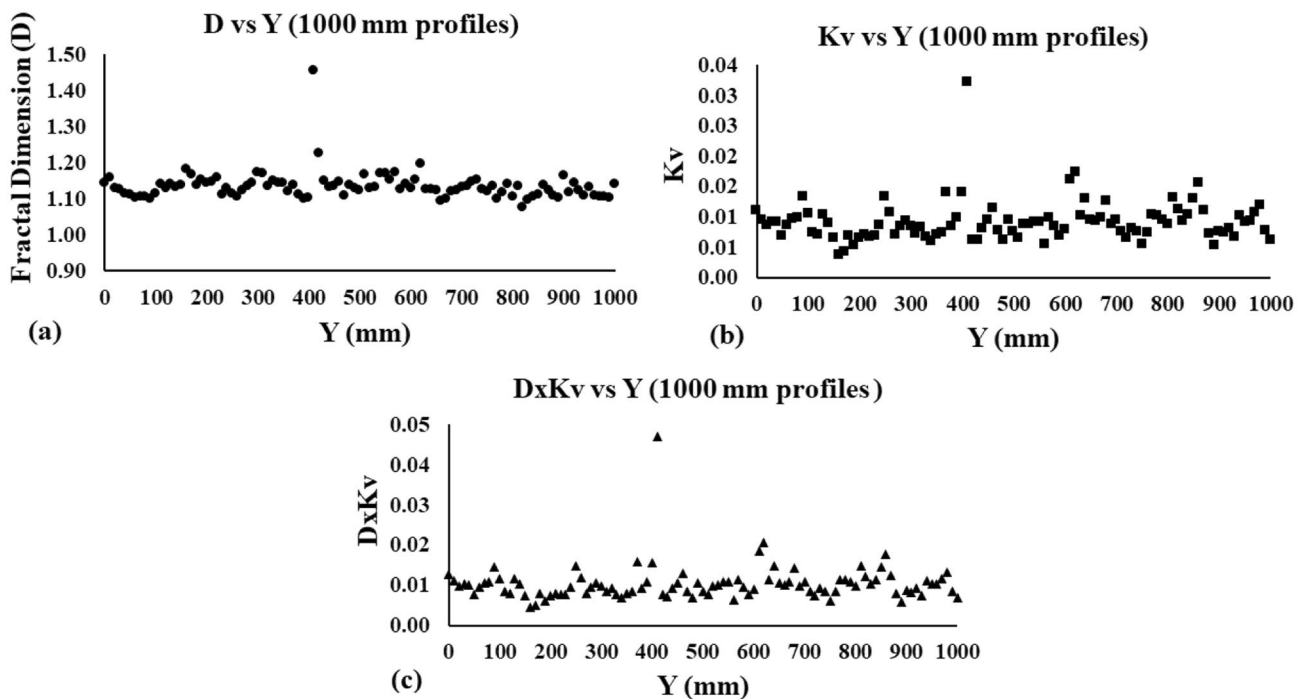
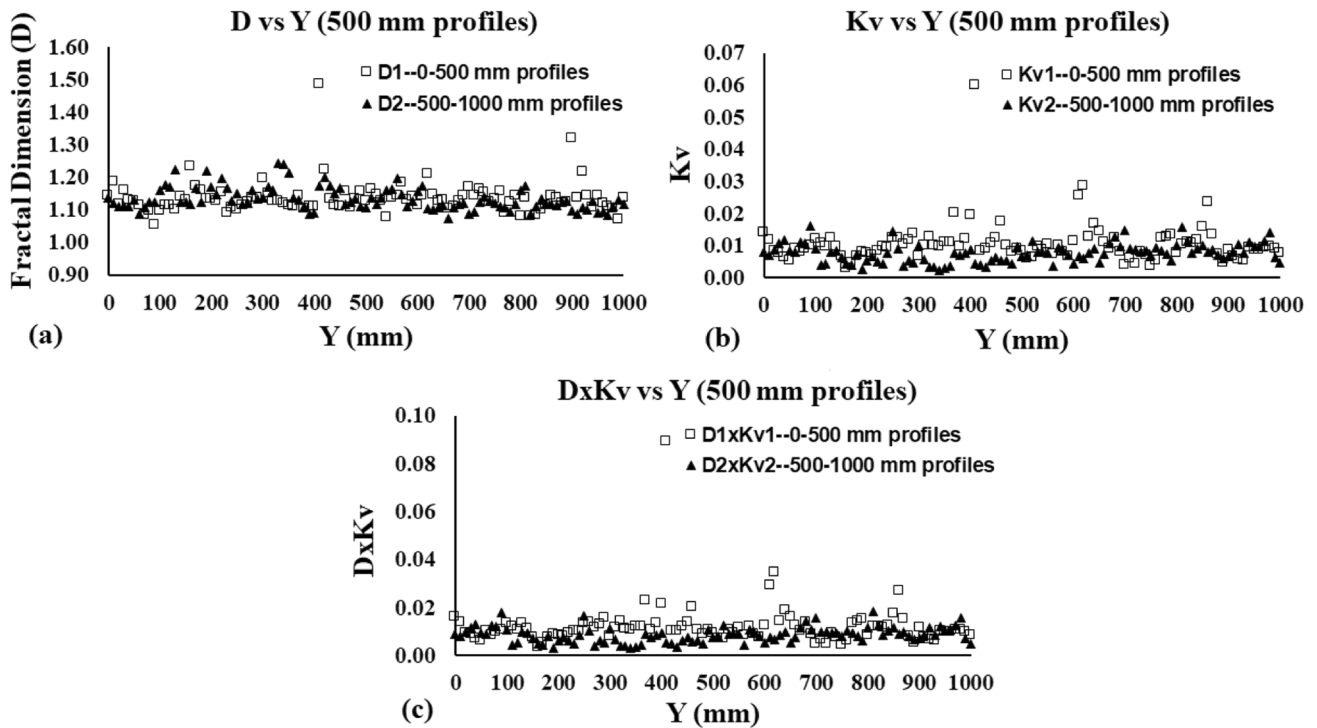**Fig. 6** Results obtained for different fractal parameters for 1000 mm Z-X profiles: **a** D; **b** K_v; **c** DxK_v

Fig. 7 Results obtained for different fractal parameters for 500 mm Z-X profiles: **a** D; **b** K_v; **c** DxK_v
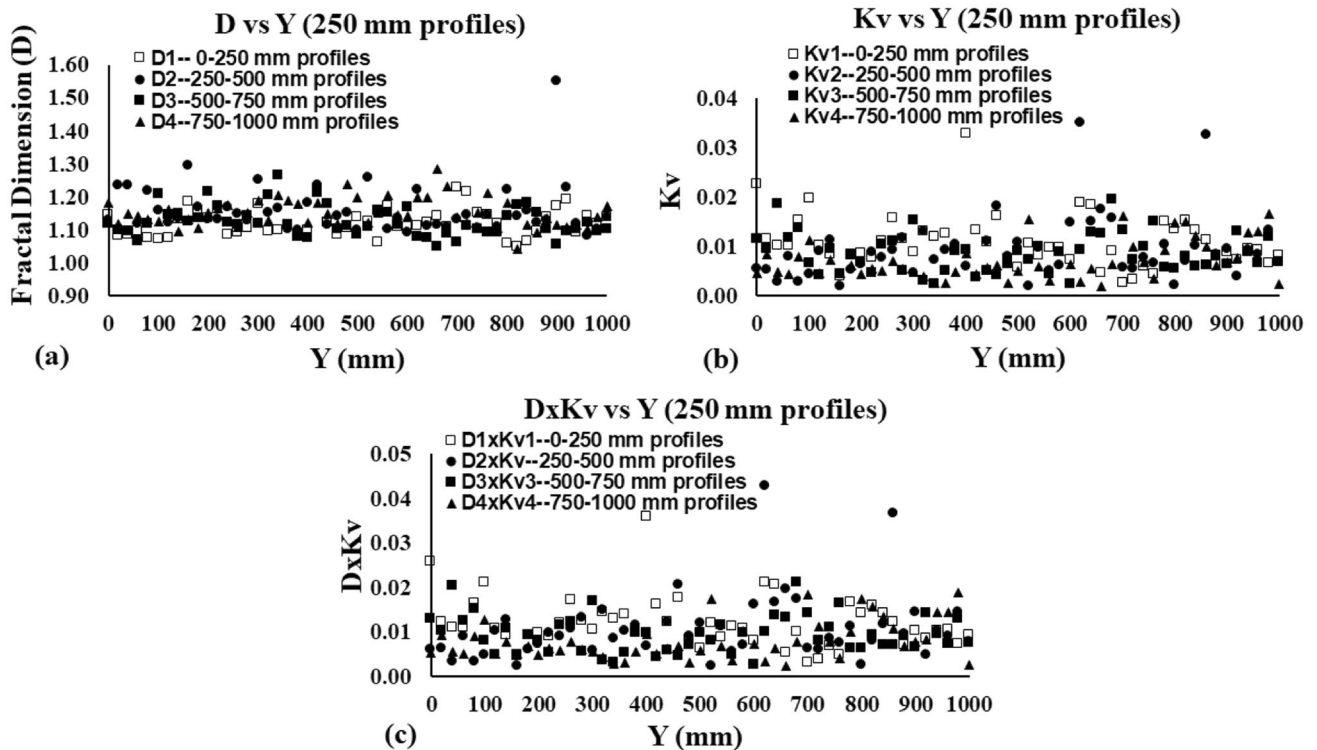

Fig. 8 Results obtained for different fractal parameters for 250 mm Z-X profiles: **a** D; **b** K_v; **c** DxK_v
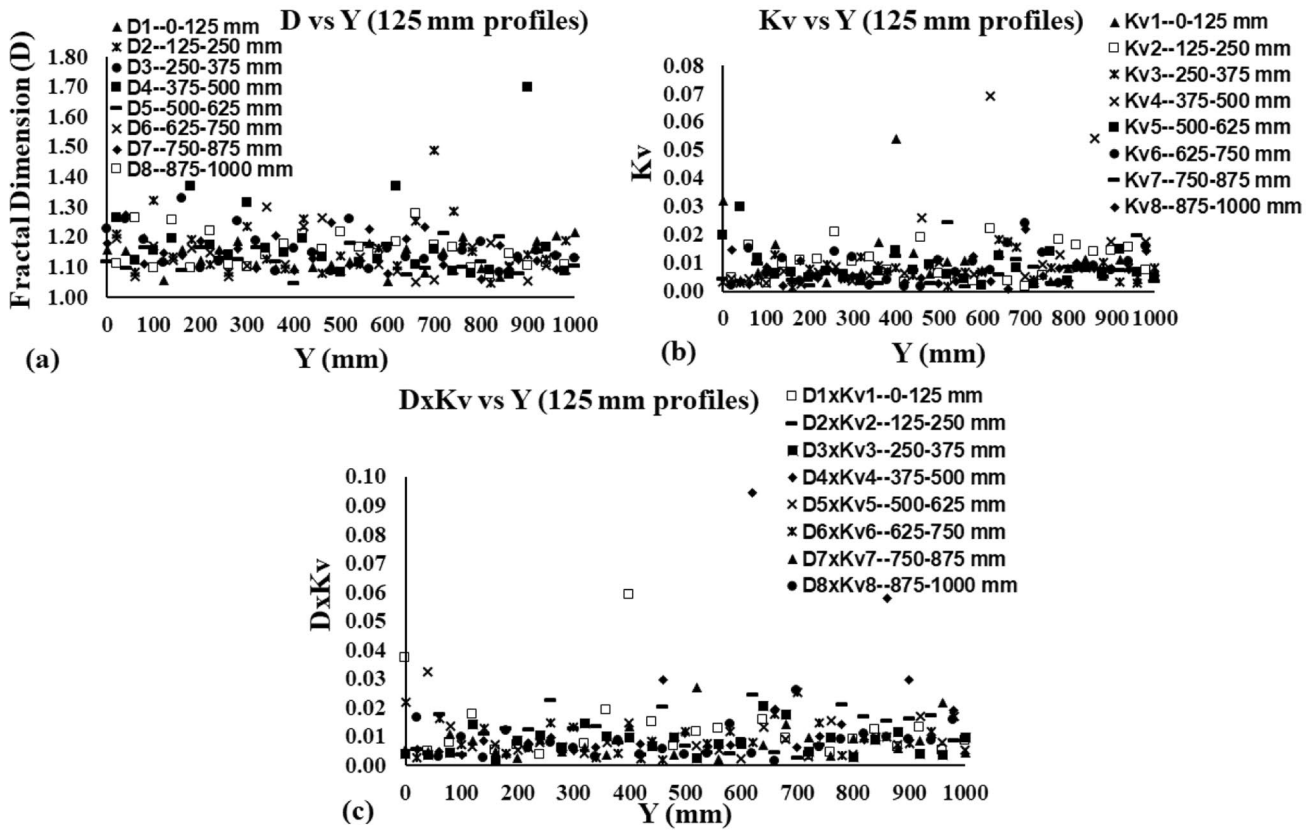
Fig. 9 Results obtained for different fractal parameters for 125 mm Z-X profiles: **a** D; **b** K_v; **c** DxK_v
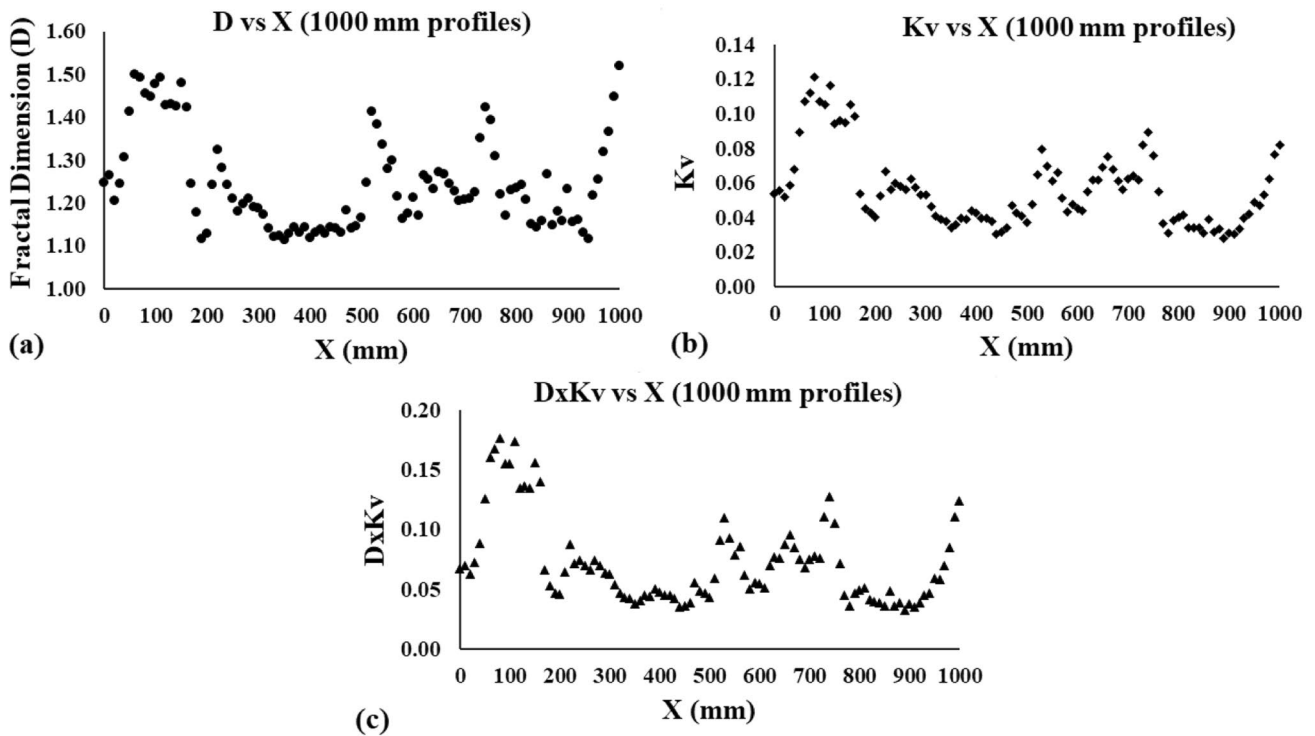

Fig. 10 Results obtained for different fractal parameters for 1000 mm Z-Y profiles: **a** D; **b** K_v; **c** DxK_v
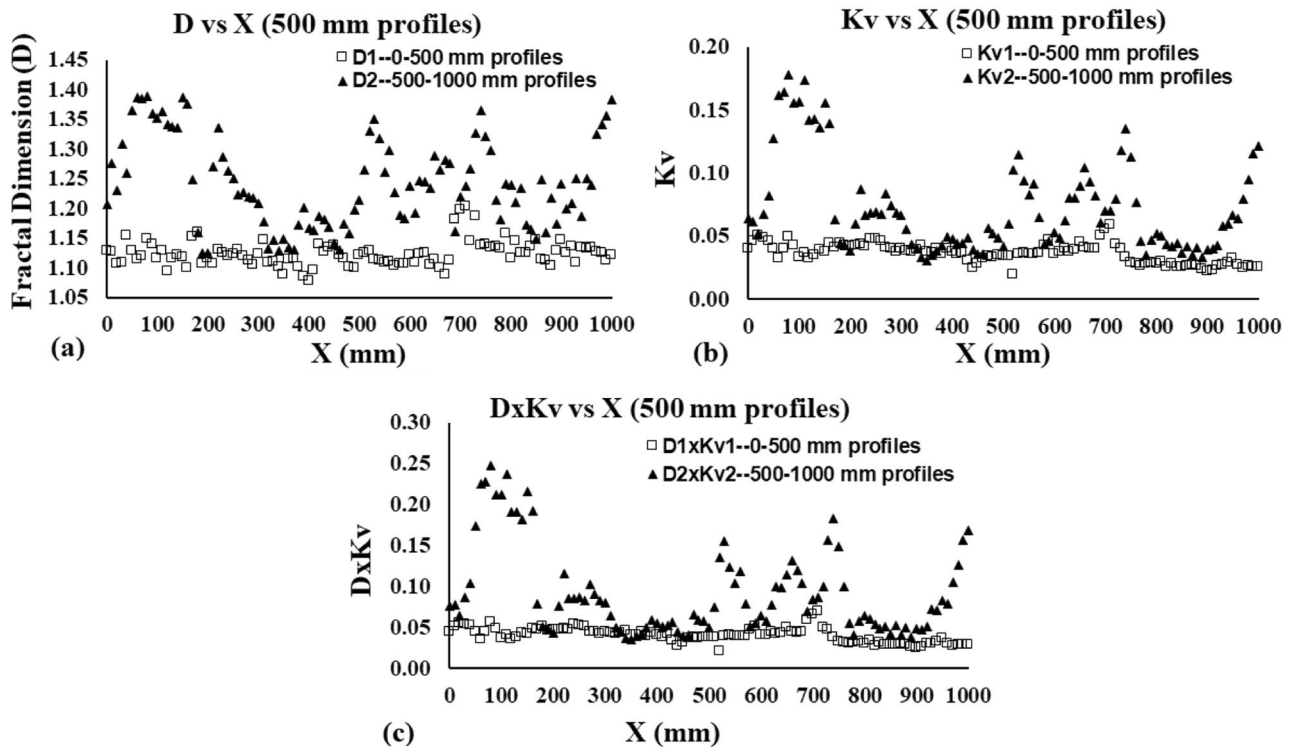
Fig. 11 Results obtained for different fractal parameters for 500 mm Z-Y profiles: **a** D; **b** K$_v$; **c** DxK$_v$
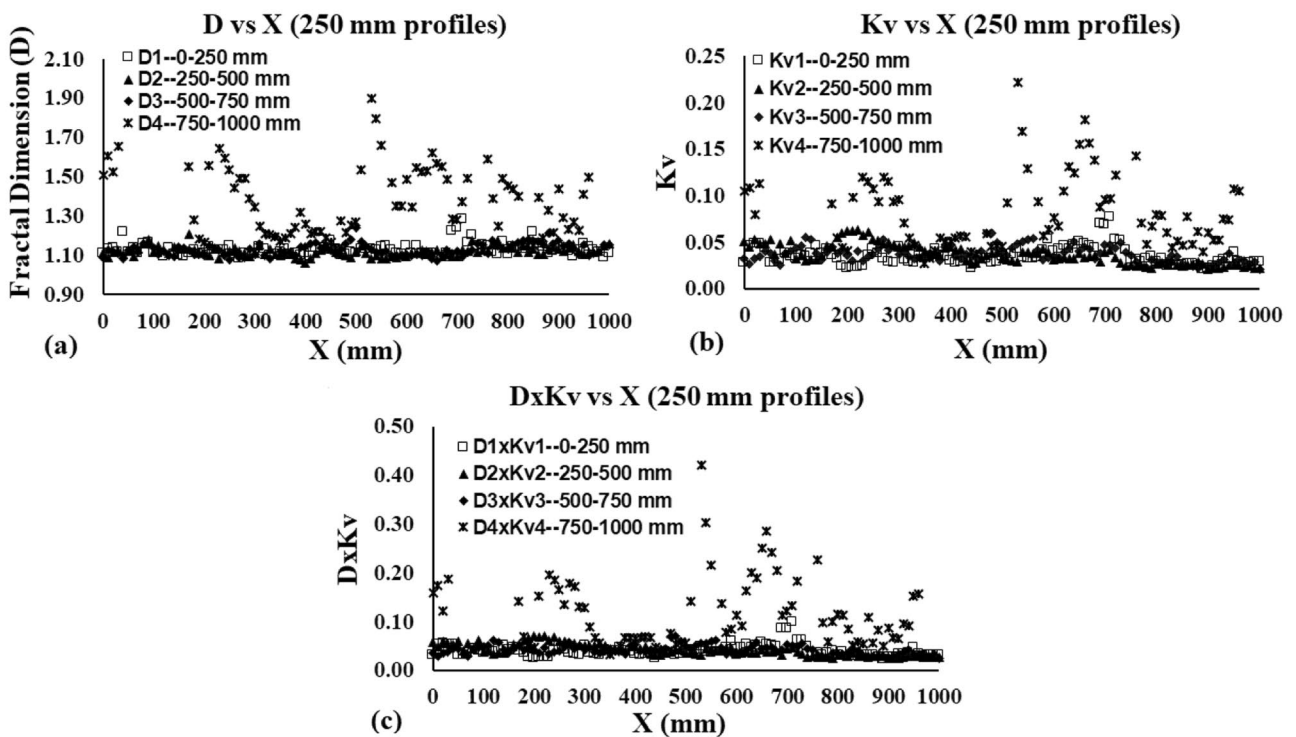

Fig. 12 Results obtained for different fractal parameters for 250 mm Z-Y profiles: **a** D; **b** K$_v$; **c** DxK$_v$

Table 3 Roughness summary statistics of results of Z–X profiles used to investigate the effect of heterogeneity on calculated variogram parameters

Case	No. of data	D			K_v			DxK_v		
		Mean	Range	CV	Mean	Range	CV	Mean	Range	CV
1000 mm Z-X profiles	101	1.1342	1.0769–1.4555	0.0352	0.0091	0.0037–0.0322	0.3714	0.0104	0.0044–0.0469	0.4418
500 mm Z-X profiles (0–500 mm)	101	1.1365	1.0537–1.4856	0.0442	0.0106	0.0029–0.0600	0.6121	0.0122	0.0036–0.0891	0.7457
500 mm Z-X profiles (500–1000 mm)	101	1.1335	1.0743–1.2440	0.0308	0.0076	0.0025–0.0160	0.3794	0.0086	0.0031–0.0185	0.3715
250 mm Z-X profiles (0–250 mm)	51	1.1220	1.0504–1.2284	0.0377	0.0108	0.0025–0.0328	0.4857	0.0121	0.0031–0.0360	0.4751
250 mm Z-X profiles (250–500 mm)	51	1.1598	1.0820–1.5507	0.0638	0.0092	0.0018–0.0351	0.6837	0.0106	0.0024–0.0429	0.6898
250 mm Z-X profiles (500–750 mm)	51	1.1249	1.0483–1.2648	0.0402	0.0085	0.0023–0.0194	0.4585	0.0094	0.0027–0.0211	0.4405
250 mm Z-X profiles (750–1000 mm)	51	1.1515	1.0433–1.2853	0.0375	0.0071	0.0018–0.0165	0.5461	0.0080	0.0024–0.0188	0.5289
125 mm Z-X profiles (0–125 mm)	26	1.1365	1.0528–1.2138	0.0413	0.0108	0.0030–0.0539	0.9736	0.0122	0.0035–0.0591	0.9564
125 mm Z-X profiles (125–250 mm)	25	1.1689	1.0459–1.4900	0.0821	0.0105	0.0018–0.0220	0.5769	0.0118	0.0027–0.0244	0.5543
125 mm Z-X profiles (250–375 mm)	26	1.1588	1.0823–1.3283	0.0528	0.0073	0.0014–0.0183	0.5761	0.0083	0.0018–0.0207	0.5627
125 mm Z-X profiles (375–500 mm)	25	1.1832	1.0746–1.6967	0.1124	0.0132	0.0027–0.0690	1.1709	0.0158	0.0037–0.0943	1.2475
125 mm Z-X profiles (500–625 mm)	26	1.1313	1.0490–1.2133	0.0363	0.0087	0.0020–0.0297	0.6774	0.0098	0.0023–0.0327	0.6627
125 mm Z-X profiles (625–750 mm)	25	1.1307	1.0511–1.2989	0.0568	0.0089	0.0016–0.0240	0.6190	0.0098	0.0020–0.0253	0.5889
125 mm Z-X profiles (750–875 mm)	26	1.1515	1.0599–1.2727	0.0470	0.0074	0.0018–0.0246	0.6925	0.0084	0.0022–0.0272	0.6676
125 mm Z-X profiles (875–1000 mm)	25	1.1553	1.0749–1.2773	0.0491	0.0073	0.0011–0.0221	0.6595	0.0082	0.0014–0.0260	0.6557

Table 4 Roughness summary statistics of results of Z-Y profiles used to investigate the effect of heterogeneity on calculated variogram parameters

Case	No. of data	D			K_v			DxK_v		
		Mean	Range	CV	Mean	Range	CV	Mean	Range	CV
1000 mm Z-Y profiles	101	1.2458	1.1124–1.5199	0.0885	0.0564	0.0281–0.1213	0.3940	0.0725	0.0326–0.1766	0.4955
500 mm Z-Y (0–500 mm) profiles	101	1.1232	1.0782–1.2026	0.0189	0.0359	0.0188–0.0584	0.2173	0.0404	0.0212–0.0703	0.2237
500 mm Z-Y (500–1000 mm) profiles	101	1.2428	1.1244–1.3887	0.0598	0.0727	0.0306–0.1782	0.5115	0.0929	0.0352–0.2475	0.5759
250 mm Z-Y (0–250 mm) profiles	101	1.1287	1.0845–1.2811	0.0291	0.0352	0.0203–0.0768	0.2877	0.0399	0.0228–0.0984	0.3132
250 mm Z-Y (250–500 mm) profiles	101	1.1183	1.0620–1.2054	0.0216	0.0368	0.0209–0.0629	0.2945	0.0411	0.0236–0.0711	0.2922
250 mm Z-Y (500–750 mm) profiles	101	1.1284	1.0693–1.2403	0.0273	0.0370	0.0212–0.0599	0.2334	0.0417	0.0245–0.0694	0.2290
250 mm Z-Y (750–1000 mm) profiles	78	1.3780	1.1327–1.9014	0.1227	0.0812	0.0275–0.2211	0.4768	0.1177	0.0322–0.4204	0.6053

Next, the results of all the profiles stated in "Effect of heterogeneity on computed D, Kv, and DxKv of roughness profiles" are used to study the effect of joint size on quantified roughness parameters. The only difference in this case compared to "Effect of heterogeneity on computed D, Kv, and DxKv of roughness profiles" is the results on each of the different length profiles coming from different sections are lumped together as shown in Tables 6 and 7 in making comparisons between the different joint sizes. For example, results of 250 mm Z-X profiles coming from the 4 Sects. (0–250 mm, 250–500 mm, 500–750 mm, and 750–1000 mm) are lumped together (see Table 6) rather than treating each section separately (see Table 3) in computing the summary statistics. Similar treatment is given to the results of 500 mm Z-X profiles, 125 mm Z-X profiles, 500 mm Z-Y profiles, and 250 mm Z-Y profiles in computing the summary statistics (see Tables 6 and 7). It is important to note that in this case, the joint size effect on roughness is evaluated under the influence of the heterogeneity of the joint surface. Note that for the 250 mm Z-Y profiles, 23 of the 404 profiles produced R (linear correlation coefficient) values less than 0.85. Therefore, those results are not included in computing the summary statistics for 250 mm Z-Y profiles (see Table 7). All other Z-Y profiles and all the Z-X profiles produced R values greater than 0.85.

Table 6 results show that for Z-X profiles, the mean values of D, K_v, and DxK_v almost remain the same with increasing joint size. For the same profiles, the CV values of D and K_v decrease with increasing joint size. This means the variability of the roughness profiles has decreased with increasing joint size. Table 7 results show that for Z-Y profiles, the mean values of D, K_v, and DxK_v slightly increase with increasing joint size. For the same profiles, the CV of D has decreased in going from 250 to 500 mm and in going from 250 to 1000 mm; however, it has not happened in going from 500 to 1000 mm. For the same profiles, the CV of K_v has decreased in going from 250 to 1000 mm and in going from 500 to 1000 mm; however, it has not happened in going from 250 to 500 mm. For the same profiles, mean of DxK_v has slightly increased with increasing joint size. On the other hand, the CV of DxK_v has decreased with increasing joint size. As far as the mean values of the roughness parameters are concerned, the results indicate little and no significant scale effect due to joint size in the Y and X directions, respectively.

In the extreme situation of a 100% smooth joint (that means a highly homogeneous joint), theoretically, there should not be any scale effect due to joint size. This means that the scale effects due to joint size should be connected to the homogeneity/heterogeneity of roughness. In natural rough rock joints, the scale effect due to the joint size should diminish as homogeneity of roughness increases. Relatively homogeneous sections used in Table 5 resulted

Table 5 Effect of joint size on computed roughness parameter summary statistics through comparison of roughness analyses results between the homogeneous lumped 0–250 mm and 250–500 mm sections of Z-Y profiles and 0–500 mm section of Z-Y profiles

Case	No. of Data	D			K_v			DxK_v		
		Mean	Range	CV	Mean	Range	CV	Mean	Range	CV
500 mm Z-Y (0–500 mm) profiles	101	1.1232	1.0782–1.2026	0.0189	0.0359	0.0188–0.0584	0.2173	0.0404	0.0212–0.0703	0.2237
250 mm Z-Y (0–250, 250–500 mm) profiles (lumped)	202	1.1235	1.0620–1.2811	0.0261	0.0360	0.0203–0.0768	0.2922	0.0405	0.0228–0.0984	0.3030

in almost no scale effect due to joint size. Also, note that the two categories in Table 5 produced low mean and CV values. The 750–1000 mm section of Z-Y profiles was found to be significantly heterogeneous and rougher compared to the 0–750 mm section. Due to that 750–1000 mm section produced the highest mean values and highest CV values for all the roughness parameters covering all joint sizes (see Table 4). This 750–1000 mm section of Z-Y profiles got combined with relatively homogeneous and less rougher sections when the joint size increased from 250 to 500 mm and from 500 to 1000 mm. Accordingly, the sections that included this higher rough 750–1000 mm Sect. (500–1000 mm and 0–1000 mm sections of Z-Y profiles) produced relatively higher mean values and higher CV values compared to the homogeneous Sects. (0–250 mm, 250–500 mm, 500–750 mm, and 0–500 mm sections of Z-Y profiles) (see Table 4). When the results of all sections of 250 mm Z-Y profiles and all sections of 500 mm Z-Y profiles are lumped together separately, only little or insignificant scale effect due to joint size exist (Table 7). On the other hand, when the results of different sections of 250 and 500 mm of Z-Y profiles are considered separately,

interpretation of the scale effect due to joint size is difficult due to the high variability of values among the different heterogeneous sections belonging to the same joint size (Table 4). Z-X profiles show much less heterogeneity compared to Z-Y profiles. Therefore, whether the results from different 125 mm, 250 mm, and 500 mm sections are lumped together or treated separately, the scale effects do not seem to exist for Z-X profiles (see Tables 3 and 6). All these observations indicate that roughness heterogeneity/homogeneity controls the presence or absence of scale effect due to joint size. Effect of heterogeneity on the computed roughness values may be the primary reason for existence of controversial findings on scale effects of roughness in the rock mechanics or engineering geology literature.

Relation between visual roughness and computed D, K_v, and DxK_v of roughness profiles

Results obtained for different profile lengths of Z-X and Z-Y showed different ranges for D, K_v, and DxK_v values (Tables 6 and 7). The reason for this is the variability of roughness among the different profiles under each of

Table 6 Roughness summary statistics of results for Z-X profiles to investigate scale effect of roughness due to joint size (including the influence of heterogeneity)

Case	No. of Data	D			K_v			DxK_v		
		Mean	Range	CV	Mean	Range	CV	Mean	Range	CV
1000 mm Z-X profiles	101	1.1342	1.0769–1.4555	0.0352	0.0091	0.0037–0.0322	0.3714	0.0104	0.0044–0.0469	0.4418
500 mm Z-X profiles	202	1.1350	1.0537–1.4856	0.0381	0.0091	0.0025–0.0600	0.5736	0.0104	0.0031–0.0891	0.6770
250 mm Z-X profiles	204	1.1395	1.0433–1.5507	0.0486	0.0089	0.0018–0.0351	0.5750	0.0100	0.0024–0.0429	0.5689
125 mm Z-X profiles	204	1.1519	1.0459–1.6967	0.0664	0.0092	0.0011–0.0690	0.8933	0.0105	0.0014–0.0943	0.9305

Table 7 Roughness summary statistics of results for Z-Y profiles to investigate scale effect of roughness due to joint size (including the influence of heterogeneity)

Case	No. of Data	D			K_v			DxK_v		
		Mean	Range	CV	Mean	Range	CV	Mean	Range	CV
1000 mm Z-Y profiles	101	1.2458	1.1124–1.5199	0.0885	0.0564	0.0281–0.1213	0.3940	0.0725	0.0326–0.1766	0.4955
500 mm Z-Y profiles	202	1.1830	1.0782–1.3887	0.0685	0.0543	0.0188–0.1782	0.5995	0.0666	0.0212–0.2475	0.6974
250 mm Z-Y profiles	381	1.1769	1.0620–1.9014	0.1107	0.0455	0.0203–0.2211	0.5866	0.0566	0.0228–0.4204	0.8101

the profile lengths of Z-X and Z-Y. The values of CV clearly indicate that the relative variation of K_v is higher than that of D. That means accurate quantification of K_v plays a more important role than D with respect to quantification of roughness of natural rock joints. D, K_v, and DxK_v are expected to increase with the roughness of the profile. As stated before, D is a measure of auto correlation of a roughness profile. Visually, D can be considered as a measure of frequency of fluctuations (up and down changes) of a roughness profile. Higher D values are associated with higher frequencies of fluctuations. K_v is a measure of the amplitude of the roughness profile. Higher K_v values are expected for higher amplitudes. Because D and K_v capture different and somewhat independent properties of the roughness profiles, a combination of both D and K_v should be used to quantify the roughness of rock joints. DxK_v is simply a combined measure of D and K_v to capture the overall roughness. Figures 13, 14, 15, and 16 provide a few roughness profiles each covering from lowest roughness

(at the top) to highest roughness (at the bottom) for different lengths of Z-X profiles. Figures 17, 18, and 19 provide a few roughness profiles each covering from lowest roughness (at the top) to highest roughness (at the bottom) for different lengths of Z-Y profiles. The computed D, K_v, and DxK_v are also given for each profile shown in Figs. 13, 14, 15, 16, 17, 18, and 19. All these figures are used to try and correlate visual roughness to computed D, K_v, and DxK_v values. The authors are convinced it worked. Hope the readers can see the D, K_v, and DxK_v values increase with increasing visual roughness of the roughness profiles.

Effect of anisotropy on computed D, K_v, and DxK_v of roughness profiles

Table 6 provides the summary statistics for D, K_v, and DxK_v parameters for different lengths of Z-X profiles. Table 7 provides the summary statistics for D, K_v, and DxK_v parameters for different lengths of Z-Y profiles.
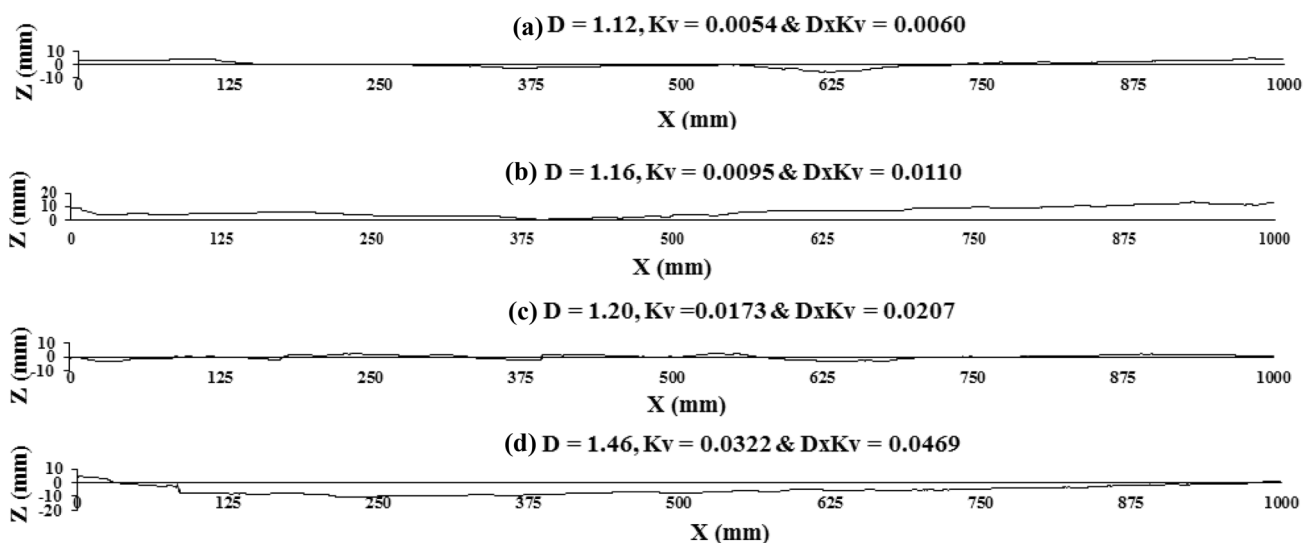
Fig. 13 Showing influence of visual roughness on the computed D, K_v, and DxK_v values using a few 1000 mm Z-X profiles
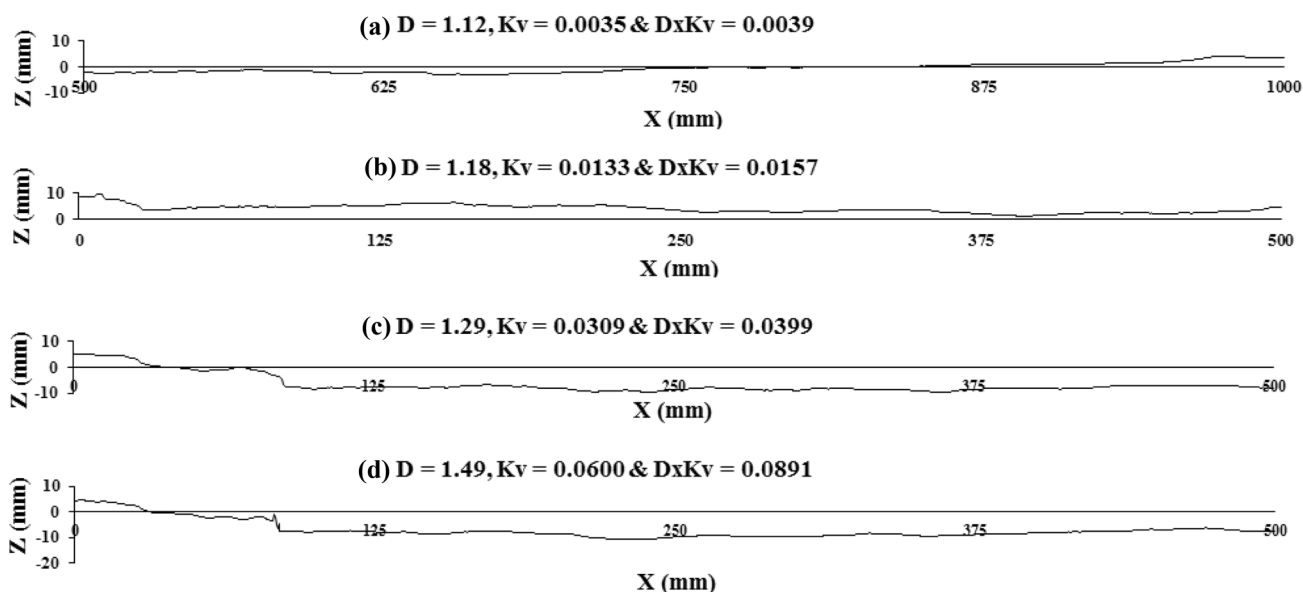
Fig. 14 Showing influence of visual roughness on the computed D, K_v, and DxK_v values using a few 500 mm Z-X profiles
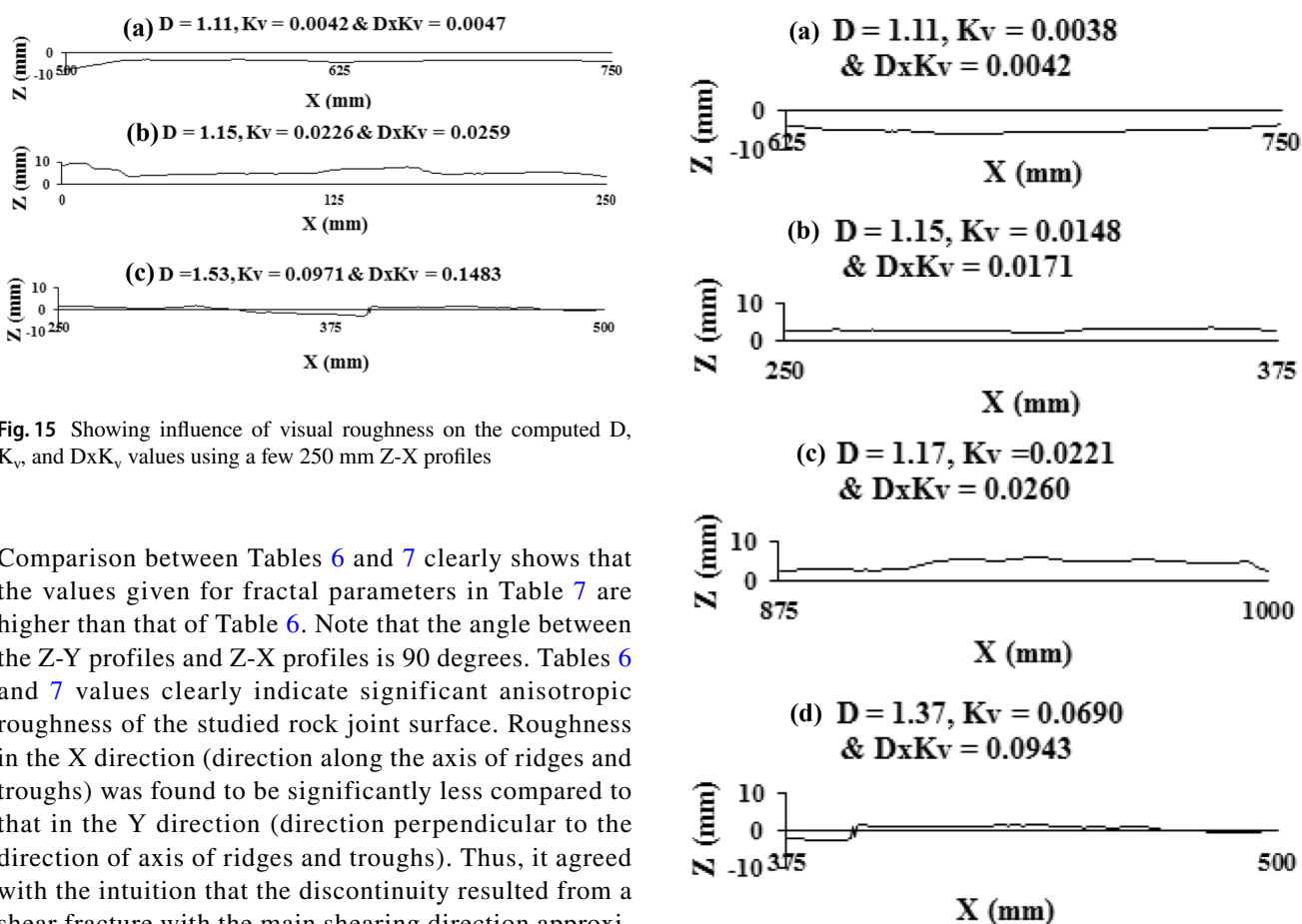

Fig. 15 Showing influence of visual roughness on the computed D, K_v, and DxK_v values using a few 250 mm Z-X profiles

Comparison between Tables 6 and 7 clearly shows that the values given for fractal parameters in Table 7 are higher than that of Table 6. Note that the angle between the Z-Y profiles and Z-X profiles is 90 degrees. Tables 6 and 7 values clearly indicate significant anisotropic roughness of the studied rock joint surface. Roughness in the X direction (direction along the axis of ridges and troughs) was found to be significantly less compared to that in the Y direction (direction perpendicular to the direction of axis of ridges and troughs). Thus, it agreed with the intuition that the discontinuity resulted from a shear fracture with the main shearing direction approximately parallel to the X direction.

Fig. 16 Showing influence of visual roughness on the computed D, K_v, and DxK_v values using a few 125 mm Z-X profiles
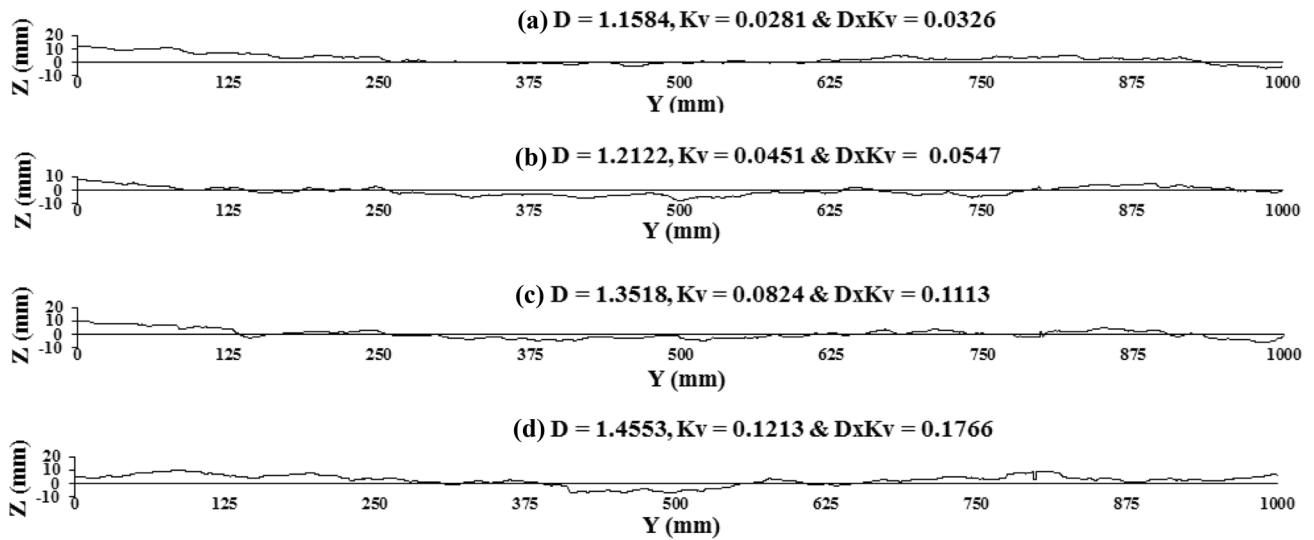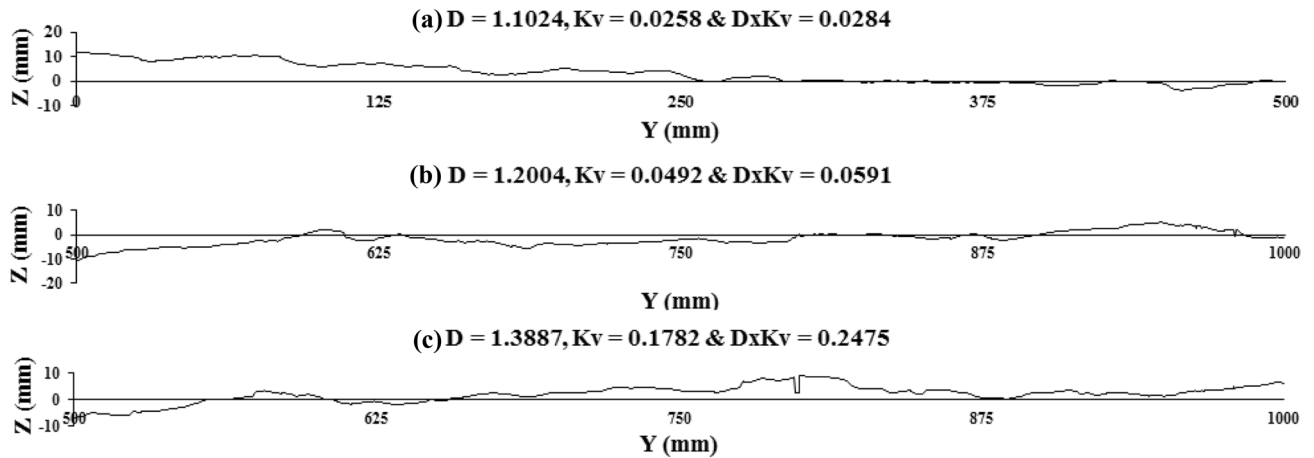
(a) D = 1.1584, Kv = 0.0281 & DxKv = 0.0326

(b) D = 1.2122, Kv = 0.0451 & DxKv = 0.0547

(c) D = 1.3518, Kv = 0.0824 & DxKv = 0.1113

(d) D = 1.4553, Kv = 0.1213 & DxKv = 0.1766

Fig. 17 Showing influence of visual roughness on the computed D, K_v, and DxK_v values using a few 1000 mm Z-Y profiles

(a) D = 1.1024, Kv = 0.0258 & DxKv = 0.0284

(b) D = 1.2004, Kv = 0.0492 & DxKv = 0.0591

(c) D = 1.3887, Kv = 0.1782 & DxKv = 0.2475

Fig. 18 Showing influence of visual roughness on the computed D, K_v, and DxK_v values using a few 500 mm Z-Y profiles

(a) D = 1.1022, Kv = 0.0254, DxKv = 0.0279

(b) D = 1.2124, Kv = 0.0407, DxKv = 0.0494
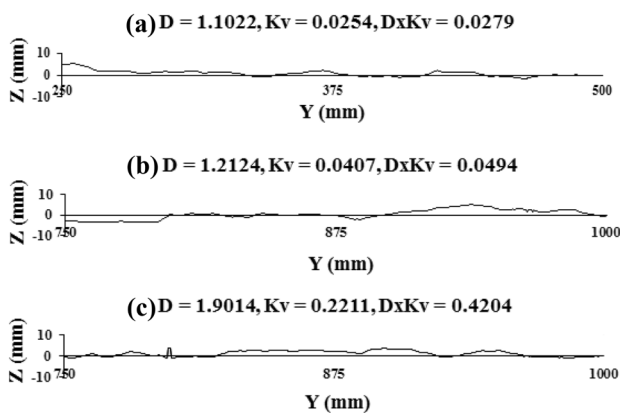
(c) D = 1.9014, Kv = 0.2211, DxKv = 0.4204

Fig. 19 Showing influence of visual roughness on the computed D, K_v, and DxK_v values using a few 250 mm Z-Y profiles

Conclusions

The paper provides a comprehensive review on rock joint roughness measurement and quantification procedures. One of the best fractal-based methodologies available in the literature, the variogram method, was used to quantify roughness of a 1 m × 1 m joint surface. Roughness computations were performed on more than 1700 profiles. Highly consistent results were obtained when the profile length changed from 125 mm or 250 to 1000 mm. These consistent results proved that the variogram method is one of the best methods available for accurate roughness quantification. The results also indicated that DxK_v is a reliable parameter available for accurate roughness

quantification. Non-stationarity of profiles resulting from a global linear trend (-1.9 to $+1.0$ degrees) was found to have no effect on the computed variogram fractal parameter values. The 0–250 mm, 250–500 mm, and 500–750 mm sections of Z-Y profiles were found to be relatively homogeneous. On the other hand, the 750 to 1000 mm section of Z-Y profiles was found to be highly heterogeneous compared to the 0–750 mm of Z-Y profiles. Similarly, the 0–500 mm section of Z-Y profiles was found to be relatively homogeneous. On the other hand, the 500 to 1000 mm section of Z-Y profiles was found to be significantly heterogeneous compared to the 0–500 mm section of Z-Y profiles. Relatively homogeneous sections used in Table 5 (0–250 mm and 250–500 mm sections of Z-Y versus 0–500 mm section of Z-Y) resulted in almost no scale effect due to joint size. The higher rough 750–1000 mm section of Z-Y profiles got combined with less rough homogeneous sections as the profile length increased from 250 to 500 mm and from 500 to 1000 mm of the Z-Y profiles. Only little or insignificant scale effect due to joint size resulted when the results of all sections of 250 mm Z-Y profiles and all sections of 500 mm Z-Y profiles were lumped together separately. On the other hand, when the results of different sections of 250 and 500 mm were considered separately, it was difficult to interpret the results on the scale effects due to the joint size for Z-Y profiles due to the high variability of values among the different heterogeneous sections belonging to the same joint size. Z-X profiles showed much less heterogeneity compared to Z-Y profiles. Therefore, whether the results from all 125 mm, 250 mm, and 500 mm sections were lumped together or treated separately for each joint size, the scale effects due to joint size did not show up for Z-X profiles. All these observations indicate that most probably the heterogeneity/homogeneity of the roughness surface play a major role on the scale effect due to joint size. The authors believe that if the joint surface is quite homogeneous, there should not be any roughness scale effect due to joint size. As everyone knows, theoretically, no roughness scale effect due to joint size exists for a 100% smooth joint, which is an extreme homogeneity situation. Computed roughness parameter values were found to increase with increasing visual roughness of the profiles. Significant roughness anisotropy was found on the studied rock joint. Roughness in the X direction (direction along the axis of ridges and troughs) was found to be significantly less compared to that in the Y direction (direction perpendicular to the direction of axis of ridges and troughs). Thus, it agreed with the intuition that the discontinuity resulted from a shear fracture with the main shearing direction approximately parallel to the X direction.

Declarations

Competing interests The authors declare that no competing interests.

References

Aydan Ö, Shimizu Y, Kawamoto T (1996) The anisotropy of surface morphology characteristics of rock discontinuities. Rock Mech Rock Eng 29(1):47–59

Bandis S, Lumsden AC, Barton NR (1981) Experimental studies of scale effects on the shear behaviour of rock joints. Int J Rock Meck Min Sci Geomech Abstr 18(1):1–21

Barton N (1973) Review of a new shear-strength criterion for rock joints. Eng Geol 7(4):287–332

Belem T, Etienne FH, Souley M (2000) Quantitative parameters for rock joint surface roughness. Rock Mech Rock Eng 33(4):217–242

Berry MV, Lewis ZV (1980) On the Weierstrass-Mandelbrot fractal function. Proceedings of the Royal Society of LondonSeries A 370(1743):459–484

Brown SR (1995) Simple mathematical model of a rough fracture. J Geophys Res 100(B4):5941–5952

Brown SR, Scholz CH (1985) Broad bandwidth study of the topography of natural rock surface. J Geophys Res 90(B14):12575–12582

Cravero M, Iabichino G, Ferrero AM (2001) Evaluation of joint roughness and dilatancy of schistosity joints. In: Sarkka P, Eloranta P (eds) Rock mechanics-a challenge for society; Proceedings of Eurock Espoo, Finland, AA Balkema, Rotterdam 217–222

Cravero M, Iabichino G, Piovano V (1995) Analysis of large joint profiles related to rock slope instabilities. In: Proceedings of the 8th ISRM Congress, Tokyo, Japan, AA Balkema, Rotterdam 423–428

Develi K, Babadagli T, Comlekci C (2001) A new computer-controlled surface-scanning device for measurement of fracture surface roughness. Comput Geosci 27(3):265–277

Du S (1998) Research on complexity of surface undulating shapes of rock joints. J China Univ Geo 9:86–89

Du S, Hu Y, Hu X (2009) Measurement of joint roughness coefficient by using profilograph and roughness ruler. J Earth Sci 20(5):890–896

Du S, Du K, Yong R, Ye J, Luo Z (2021) Scale effect on the anisotropy characteristics of rock joint roughness. Q J Eng Geol Hydrogeol. https://doi.org/10.1144/qjegh2020-066

El-Soudani SM (1978) Profilometric analysis of fractures. Metallography 11(3):247–336

Fardin N (2008) Influence of structural non-stationarity of surface roughness on morphological characterization and mechanical deformation of rock joints. Rock Mech Rock Eng 41(2):267–297

Fardin N, Feng Q, Stephansson O (2004) Application of a new in situ 3D laser scanner to study the scale effect on the rock joint surface roughness. Int J Rock Mech Min Sci 41(2):329–335

Fardin N, Stephansson O, Jing L (2001) The scale dependence of rock joint surface roughness. Int J Rock Mech Min Sci 38(5):659–669

Fecker E, Rengers N (1971) Measurement of large-scale roughness of rock planes by means of profilograph and geological compass. Rock fracture. In: Proceeding of the 1st ISRM Symposium, Nancy, France 1–18

Feder J (1988) Fractals. New York: Plenum Press 1988

Feng Q, Fardin N, Jing L, Stephansson O (2003) A new method for in-situ non-contact roughness measurement of large rock fracture surfaces. Rock Mech Rock Eng 36(1):3–25

Ge YF, Kulatilake PHSW, Tang HM, Xiong C (2014) Investigation of natural rock joint roughness. Comput Geotech 55:290–305

Grasselli G, Wirth J, Egger P (2002) Quantitative three-dimensional description of a rough surface and parameter evolution with shearing. Int J Rock Mech Min Sci 39(6):789–800

Hong ES, Lee JS, Lee IM (2008) Underestimation of roughness in rough rock joints. Int J Numer Anal Meth Geomech 32(11):1385–1403

Hsiung SM, Ghosh A, Ahola MP, Chowdhury AH (1993) Assessment of conventional methodologies for joint roughness coefficient determination. Int J Rock Mech Min Sci Geomech Abstr30:825–829

Huang SL, Oelfke SM, Speck RC (1992) Applicability of fractal characterization and modelling to rock joint profiles. Int J Rock Mech Min Sci Geomech Abstr29(2):89–98

ISRM (1978) International Society for Rock Mechanics commission on standardization of laboratory and field tests: suggested methods for the quantitative description of discontinuities in rock masses. Int J Rock Mech Min Sci Geomech Abstr 15(6):319–368

Jiang YJ, Li B, Tanabashi Y (2006) Estimating the relation between surface roughness and mechanical properties of rock joints. Int J Rock Mech Min Sci 43(6):837–846

Kodikara JK, Johnston IW (1994) Shear behaviour of irregular triangular rock -concrete joints. Int J Rock Mech Min Sci Geomech Abstr31(4):313–322

Kulatilake PHSW, Balasingam P, Park J, Morgan R (2006) Natural rock joint roughness quantification through fractal techniques. Geotech Geol Eng 24:1181–1202

Kulatilake PHSW, Park J, Morgan Balasingam P, R, (2008) Quantification of aperture and relations between aperture, normal stress and fluid flow for natural single rock fractures. Int Jour of Geotech and Geological Engg 26(3):269–281

Kulatilake PHSW, Shou G, Huang TM, Morgan RM (1995) New peak shear strength criteria for anisotropic rock joints. Int J Rock Mech Min Sci Geomech Abstr32:673–697

Kulatilake PHSW, Um J (1999) Requirements for accurate quantification of self-affine roughness using the roughness-length method. Int J Rock Mech Min Sci 36(1):5–18

Kulatilake PHSW, Um J, Pan G (1997) Requirements for accurate estimation of fractal parameters for self-affine roughness profiles using the line scaling method. Rock Mech Rock Eng 30(4):181–206

Kulatilake PHSW, Um J, Pan G (1998) Requirements for accurate quantification of self-affine roughness profiles using variogram method. Int J Solids Struct 35(31):4167–4189

Kulatilake PHSW, Um J, Panda BB, Nghiem N (1999) Development of a new peak shear strength criterion for anisotropic rock joints. J Eng Mech 125(9):1010–1017

Lanaro F (2000) A random field model for surface roughness and aperture of rock fractures. Int J Rock Mech Min Sci 37(8):1195–1210

Lanaro F, Jing L, Stephansson O (1998) 3D-laser measurements and representation of roughness of rock fractures. In: Proceeding of Mechanics of Jointed and Faulted Rock, Rotterdam 185–189

Lanaro F, Jing L, Stephansson O (1999) Scale dependency of roughness and stationarity of rock joints. In: Vouille G, Berest P (eds) Proceedings of the 9th congress of ISRM, Paris, France 1391–1395

Leal-Gomes MJA (2003) Some new essential questions about scale effects on the mechanics of rock joints. In: Handley M (ed) Proceedings of the 10th ISRM Congress: Technology roadmap for rock mechanics, Sandton, South Africa, South African Institute of Mining and Metallurgy 721–727

Maerz NH, Franklin JA, Bennett CP (1990) Joint roughness measurement using shadow profilometry. Int J Rock Mech Min Sci Geomech Abstr 27:329–343

Malinverno A (1990) A simple method to estimate the fractal dimension of a self-affine series. Geophys Res Lett 17(11):1953–1956

Mandelbrot BB (1967) How long is the coast of Britain? Statistical Self-Similarity and Fractional Dimension Science 156(3775):636–638

Matsushita M, Ouchi S (1989) On the self-affinity of various curves. Physica D 38(1):246–251

Miller SM, McWilliams PC Kerkering JC (1990) Ambiguities in estimating fractal dimensions of rock fracture surfaces. In: Proceeding of the 31st U.S. Symposium on Rock Mechanics, Rotterdam 471–478

Myers NO (1962) Characterization of surface roughness. Wear 5(3):182–189

Odling NE (1994) Natural fracture profiles, fractal dimension and joint roughness coefficient. Rock Mech Rock Eng 27(3):135–153

Orey S (1970) Gaussian simple functions and Hausdorff dimension of level crossing. Zeitschrift Für Wahrscheinlichkeitstheorie Und Verwandte Gebiete 15(3):249–256

Poon CY, Sayles RS, Jones TA (1992) Surface measurement and fractal characterization of naturally fractured rocks. J Phys D Appl Phys 25(8):1269–1275

Power WL, Tullis TE (1991) Euclidean and fractal models for the description of rock surface roughness. J Geophys Res 96(B1):415–424

Rasouli V, Harrison JP (2000) Scale effect, anisotropy and directionality of discontinuity surface roughness. Proceeding of EUROCK National Symposium for Felsmechanik Und Tunnelbau, Aachen, Germany 14:751–756

Russ JC (1994) Fractal surfaces. Springer

Sayles RS, Thomas TR (1977) The spatial representation of surface roughness by means of the structure function: a practical alternative to correlation. Wear 42(2):263–276

Shirono T, Kulatilake PHSW (1997) Accuracy of the spectral method in estimating fractal / spectral parameters for self-affine roughness profiles. Int J Rock Mech Min Sci 34(5):789–804

Swan G, Zongqi S (1985) Prediction of shear behaviour of joints using profiles. Rock Mech Rock Eng 18(3):183–212

Tatone BSA, Grasselli G (2013) An investigation of discontinuity roughness scale dependency using high-resolution surface measurements. Rock Mech Rock Eng 46(4):657–681

Tse R, Cruden DM (1979) Estimating joint roughness coefficients. Int J Rock Mech Min Sci Geomech Abstr 16(5):303–307

Wu TH, Ali EM (1978) Statistical representation of the joint roughness. Int J Rock Mech Min Sci Geomech Abstr15(5):259–262

Xie HP, Wang JA, Xie WH (1997) Fractal effects of surface roughness on the mechanical behavior of rock joints. Chaos, Solitons Fractals 8(2):221–252

Yong R, Ye J, Du LB, S, (2018) Determining the maximum sampling interval in rock joint roughness measurements using Fourier series. Int J Rock Mech Min Sci 101:78–88. https://doi.org/10.1016/j.ijrmms.2017.11.008

Yu XB, Vayssade B (1991) Joint profiles and their roughness parameters. Int J Rock Mech Min Sci Geomech Abstr28(4):333–336

Zhang X, Jiang Q, Chen N, Wei W, Feng X (2016) Laboratory investigation on shear behavior of rock joints and a new peak shear strength criterion. Rock Mech Rock Eng 49:3495–3512. https://doi.org/10.1007/s00603-016-1012-2